DEPARTMENT OF ONCOLOGY-PATHOLOGY
Karolinska Institutet, Stockholm, Sweden

FROM CELL SURVIVAL TO DOSE RESPONSE – MODELING BIOLOGICAL EFFECTS IN RADIATION THERAPY

Minna Wedenberg

Karolinska Institutet

Stockholm 2013

Published by Karolinska Institutet. Printed by Universitetsservice US-AB, Stockholm.

ISBN 978-91-7549-250-6

Till männen i mitt liv - Niklas, Oliver och Ville

Abstract

The main goal in curative radiation therapy is to eradicate the tumor while minimizing radiation-induced damage to normal tissue. Ions, including protons and carbon ions, are increasingly being used for cancer treatment. They allow for a more focused dose to the tumor and exhibit higher effectiveness in cell killing compared to conventional radiation therapy using photons. The aim of this thesis is to develop and evaluate mathematical models for biological effect estimation with the focus on proton and light ion irradiation.

Two radiobiological models for ions were developed. Firstly, the repairable-conditionally repairable damage (RCR) cell survival model was extended to account for the linear energy transfer (LET). Secondly, a model that estimates the relative biological effectiveness (RBE) of protons based on dose, LET, and cell type was derived. The LET-parameterized RCR model provides an adequate fit to experimental cell survival data derived from irradiation with carbon ions and helium ions. The RBE model predicts a cell-dependent relation between RBE and LET determined by the cell-specific parameter α/β of the linear-quadratic model of photons.

In a separate study, the effect of accounting for variable RBE in treatment plan comparison was investigated using the proposed RBE model. Lower RBE was predicted in the tumor and higher RBE in adjacent organs than the commonly assumed RBE equal to 1.1. Disregarding this variation and instead assuming RBE equal to 1.1 in treatment plan optimization may lead to optimistic estimates for the proton plan and thereby biases treatment plan comparison in its favor.

Derived dose-response relations of normal tissue toxicity are uncertain because they are based on limited numbers of patients. A bootstrap method was proposed to assess the uncertainty in clinical outcome data due to sampling variability, and translate this into an uncertainty in the dose-response relation. The method provides confidence intervals of the dose-response relation, suggests model parameter values with confidence intervals and their interrelation, and can be used for model selection.

Keywords: Radiobiological models, proton radiation therapy, carbon ion radiation therapy, relative biological effectiveness, linear energy transfer, bootstrap.

Sammanfattning

Det huvudsakliga målet med kurativ strålbehandling är att slå ut tumören utan att skada intilliggande frisk vävnad. Bestrålning med joner såsom protoner och koljoner har blivit allt vanligare inom cancerbehandling. Joner möjliggör en mer fokuserad dos till tumören och inducerar celldöd mer effektivt än traditionell strålterapi med fotoner (röntgenstrålning). Syftet med denna avhandling är att utveckla och utvärdera matematiska modeller som förutsäger den biologiska effekten av bestrålning, med fokus på proton- och jonstrålning.

Två strålbiologiska modeller för joner har utvecklats. Den första utvidgar en cellöverlevnadsmodell, RCR-modellen, genom att ta hänsyn till den linjära energiöverföringen (LET). Den andra estimerar den relativa biologiska effektiviteten för protoner baserat på dos, LET, och celltyp. Den LET-parametriserade RCR-modellen ger bra anpassning till experimentella cellöverlevnadsdata från bestrålning med kol- och heliumjoner. RBE-modellen visar att sambandet mellan RBE och LET beror av celltyp, där celltypen definieras av parametern α/β från den linjär-kvadratiska modellen för fotoner.

I ett separat arbete studerades effekten av en varierande RBE när behandlingsplaner jämförs. Med den föreslagna RBE-modellen erhölls lägre RBE i tumören och högre RBE i intilliggande riskorgan än det allmänt antagna värdet 1.1. Optimering utan hänsyn till RBE-variation kan ge en sämre protonplan än förväntat, om RBE skiljer sig från det antagna värdet 1.1, vilket kan snedvrida jämförelser av planer.

Empiriskt härledda dos-responsrelationer för vävnadstoxicitet är osäkra eftersom de utgår från ett begränsat antal patienter. En bootstrap-metod föreslås för att uppskatta osäkerheten i klinisk utfallsdata som följd av variansen i stickprovet och omvandla detta till en osäkerhet i dos-responsrelationer. Metoden ger modellparameterskattningar med konfidensintervall och inbördes beroende, konfidensintervall for dos-responsrelationer, och stöd för modellval.

Nyckelord: Strålbiologiska modeller, protonterapi, koljonsterapi, relativ biologisk effektivitet, linjär energiöverföring (LET), bootstrap.

List of papers

This thesis is based on the following original publications, which are referred to in the text by their Roman numerals.

I Wedenberg, M., Lind, B. K., Toma-Dasu, I., Rehbinder, H, Brahme, A. (2010). Analytical description of the LET dependence of cell survival using the Repairable-Conditionally Repairable damage model. *Radiation Research*, 174:517-525.

II Wedenberg, M., Lind, B. K., Hårdemark, B. (2013). A model for the relative biological effectiveness of protons: The tissue specific parameter α/β of photons is a predictor for the sensitivity to LET changes. *Acta Oncologica*, 52:580–588.

III Wedenberg, M., Toma-Dasu, I. (2013). Disregarding RBE variation in treatment plan comparison may lead to bias in favor of proton therapy. *Submitted for publication*.

IV Wedenberg, M. (2013). Assessing the uncertainty in QUANTEC's dose-response relation of lung and spinal cord with a bootstrap analysis. *International Journal of Radiation Oncology, Biology, Physics*, Published online: http://dx.doi.org/10.1016/j.ijrobp.2013.06.2040.

Reprints of **I**, **II**, and **IV** were made with kind permission from the publishers.

Table of Contents

Abbreviations

3DCRT	Three Dimensional Conformal Radiation Therapy
AIC	Akaike Information Criterion
BED	Biologically Effective Dose
BIC	Bayesian Information Criterion
CT	Computed Tomography
CTV	Clinical Target Volume
DVH	Dose Volume Histogram
EQD	Equivalent Dose
EUD	Equivalent Uniform Dose
GTV	Gross Tumor Volume
ICRU	International Commission on Radiation Units and Measurements
IMPT	Intensity Modulated Proton Therapy
IMRT	Intensity Modulated Radiation Therapy
LET	Linear Energy Transfer
LKB model	Lyman Kutcher Burman Model
LQ model	Linear-Quadratic Model
LSE	Least Square Estimation
MLC	Multileaf Collimator
MLE	Maximum Likelihood Estimation
NTCP	Normal Tissue Complication Probability
OAR	Organ At Risk
PTV	Planning Target Volume
QUANTEC	Quantitative Analysis of Normal Tissue Effects in Clinics
RBE	Relative Biological Effectiveness
RCR model	Repairable Conditionally Repairable Damage Model
ROI	Region Of Interest
TCP	Tumor Control Probability

Introduction

In 1895, the physicist Wilhelm Conrad Röntgen discovered 'a new kind of ray' that he called x-rays; the x representing the unknown. Within a year, radiation was used to treat cancer and Röntgen was awarded the very first Nobel Prize in physics in 1901 for his discovery. Over the years, radiation therapy has developed greatly. Some of the most important technological advances include the introduction of linear accelerators in the 1960s that allowed for higher energies and thus deeper tissue penetration compared to the Cobalt machines. With computed tomography (CT), clinically available from the 1970s, three-dimensional images of the patient anatomy were obtained. This technology has made it possible to better determine the size, location, and density of tumors and normal tissue, and to align the beams accordingly. The use of computers in *e.g.* treatment optimization and dose calculation has revolutionized radiation therapy. The invention of intensity modulated radiation therapy (IMRT) (Brahme et al., 1982; Brahme, 1988) was an important step in the direction of improving the delivered dose distribution to conform the dose to the tumor. Another approach to focus the dose to the tumor has been to, instead of x-rays, use protons and heavier ions. This was first realized by Robert Wilson in 1946, and is described in his paper with the title Radiological use of fast protons (Wilson et al., 1946). The first patient was treated with protons in 1954 in Berkeley, USA. Proton radiation therapy commenced in Europe in 1957 in Uppsala, Sweden. In Berkeley, patients were treated with helium ion starting from 1975 (Saunders et al., 1985), and later also heavier ions such as neons (Castro et al., 1982, 1994).

Today radiation therapy is one of the most common ways to treat cancer along with surgery and chemotherapy. Often a combination of treatments is applied. Cancer is a leading cause of death in the world (WHO, 2013). It is a term for a group of various diseases that involve uncontrolled cell division. Normal cells may turn cancerous after accumulating several mutations in genes that control cell proliferation leading to a disruption in the normal balance between proliferation and cell death.

The resulting uncontrolled cell division can lead to a mass of cells – a tumor. Early in its development, when the tumor is generally well localized, and also when regional spread has occurred or when the tumor is inseparable from vital organs or tissues, radiation therapy may be indicated. About one in three people in Sweden will suffer from cancer during the course of their life, and about half of the patients are treated with radiation therapy (Cancerfonden, 2013).

The fundamental challenge in radiation therapy, as in all cancer treatment, is to find the right balance between eradicating the cancer and avoiding unacceptable injury to normal tissue. Most radiation therapy treatments today are given using photons, but there is an increasing interest in protons and carbon ions as reflected by the growing number of proton and carbon ion radiation therapy centers. These particles allow for a more focused dose to the tumor and higher efficiency in cell killing. The term *ion* will in this thesis mainly refer to protons (hydrogen ions) and carbon ions.

Radiation physics

Ionizing radiation refers to radiation with energy high enough to overcome the electron-binding energy in an atom or molecule. Every radiation type has its own characteristic distribution of energy depositions. The distribution affects the induction of physical, chemical and biological changes. Two important physical quantities in radiation therapy that affect the biological outcome are the absorbed dose and the linear energy transfer (LET).

Depth dose distribution

The important quantity absorbed dose is defined as the expectation value of the energy imparted by ionizing radiation to matter per unit mass at a point of interest (ICRU, 1980). It is expressed in units of Gray (Gy) where 1 Gy = 1 J/kg.

High energetic photons used in radiation therapy such as x-rays lose energy to the traversed materia mainly by three processes: 1) photoelectric effect, in which the photon interacts with a bound inner shell electron in an atom of the traversed materia and transfers its total energy to the electron which is emitted; 2) Compton scattering, in which the photon interacts with an outer orbital electron and transfers part of its energy to the emitting electron, after which the photon is scattered with reduced energy; and 3) pair production, in which the photon energy is converted to the mass and kinetic energy of an electron-positron pair. The likelihood of each of these processes depends on the energy of the photon and the atomic number

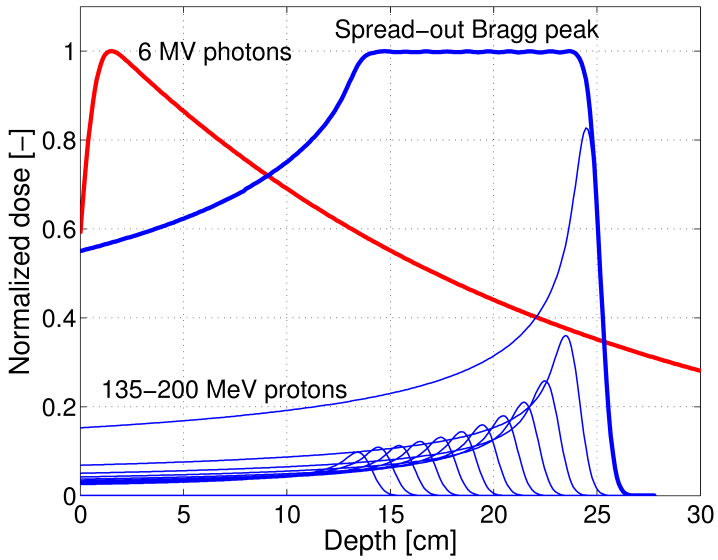

Figure 1: Depth dose profiles for broad beams of 6 MV photons and 135-200 MeV protons. By superpositioning several Bragg peaks of different energies, a spread-out Bragg peak is produced. (Courtesy of Albin Fredriksson.)

of the target atom. The emitted electrons in the different processes lose energy in turn by further ionization and excitation events. A typical photon depth dose curve, the dose distribution on the central axis, in a patient shows a low surface dose giving a so-called skin sparing effect. The dose is ”built-up” by secondary electrons and increases with depth to a maximum, at a depth (a few millimeters to a few centimeters) depending mainly on the beam energy, and then decreases almost exponentially until the beam exit point (see Figure 1).

Except for very superficial tumors, it is not opportune to treat with a single photon beam. The proximal dose in the normal tissue would be higher than the dose delivered to the tumor, and the dose beyond the tumor would also be too high. Instead multiple beams from several directions are combined.

High-energetic ions, on the other hand, interact with tissue mainly through Coulomb interactions with the atomic electrons of the material. The energy loss per unit path length of a particle, referred to as the stopping power, depends on the electron density of the traversed medium, the atomic number of the ion, the velocity of the ion, and the effective charge of the ion. Since the rate of energy

transfer is inversely proportional to the square of the velocity of the ion, the energy deposition is small at high velocities. As a consequence, the deposited dose is low at small depths where the ions have their highest energy. As the ions slow down, the dose increases with depth and forms a sharp maximum at the end of the range, the Bragg peak. For protons, the fall-off in energy depositions beyond the Bragg peak is sharp. With increasing atomic number of the ion, nuclear fragmentation increases causing energy depositions beyond the Bragg peak forming a so called fragmentation tail. Thus, for carbon ions some dose is deposited beyond the peak. The height of the Bragg peak depends on the mass of the ions, and the range of an ion, and thus the location of the Bragg peak, is determined by the initial energy. At the depth of the Bragg peak there is a spread of energies due to fluctuations between ions in the number of collisions and transferred energies. This is known as range straggling or energy-loss straggling. In summary, a low dose is obtained at the entrance, the dose peaks at the end of the track, and very little dose is deposited behind the peak. This feature of ions is utilized in radiation therapy to obtain a more focused dose to deep-seated tumors than would be possible with photons, while lowering the dose to the normal tissue.

The width of a Bragg peak is too small to cover an entire tumor. By superpositioning several Bragg peaks of different energies a so called spread-out Bragg peak is obtained, shown in Figure 1.

Linear energy transfer

In ion irradiation, not only the amount of energy deposited in a volume (the dose) is of importance but also how the energy depositions are distributed. The spatial distribution of energy depositions influences the effectiveness in producing radiation-induced changes. One way of characterizing this local energy spectrum is by the linear energy transfer, LET. LET is closely related to the collision stopping power and is a measure of the average energy locally imparted to the material by a charged particle per unit length of the particle track (ICRU, 1970)

$$L_\Delta = \left(\frac{\mathrm{d}E}{\mathrm{d}l} \right)_\Delta \tag{1}$$

where $\mathrm{d}E$ is the mean energy loss due to collisions with energy transfers less than a cut-off value Δ, and $\mathrm{d}l$ is the distance traversed by the particle. Whereas stopping power focuses on the energy loss of the particle, LET focuses on the energy absorbed by the material. The cut-off value Δ is an energy limit to restrict to energy

losses occurring "locally" by excluding secondary electrons with energies exceeding Δ. In the unrestricted LET, L_∞, all possible energy transfers are included.

LET is useful for defining the quality of ionizing radiation. A distinction between low- and high-LET radiation is often made. Low-LET radiation, or sparsely ionizing radiation, such as electrons, experience many interactions with material and the ionizations produced are distributed over a relatively long path resulting in a low ionization density. ^{60}Co γ-rays or x-rays are usually also referred to as low-LET radiation, although the definition of LET is limited to charged particles, since the electrons generated from photon interactions have generally low LET. In contrast, high-LET radiation, such as carbon ions, deposit a large amount of energy in a small distance and produce in that way more clustered, and thereby more severe, DNA damage. Protons may produce high LET in the Bragg peak but belong generally to radiation of low LET.

In most experimental situations, there is a distribution of LET values. An average LET at every position can be calculated and the two most common measures are the dose averaged LET and the track (or fluence) averaged LET. A dose averaged LET can be calculated by weighting the LET contribution of each proton by the dose it deposits, and a track averaged LET is obtained by weighting the LET by the number of particles, *i.e.* it is the arithmetic mean LET.

LET is one of the descriptors of the radiation quality and has been found to correlate with the relative biological effectiveness. Alternative measures of radiation quality might be the number of ionizations per path length, or the microdosimetric quantity dose-mean linear energy. A measure that more uniquely describes the radiation quality would be beneficial.

Radiation biology

Radiation biology, or radiobiology, is the study of the effects of radiation on living systems. Absorbed radiation dose is an important quantity when predicting the biological effect. However, there are many factors that affect the biological response to a given dose: the inherent radiosensitivity of the biological system studied, the degree of oxygenation, the dose distribution within the irradiated volume, the way dose is fractionated, *e.g.* dose per fraction, the time between fractions, overall treatment time, etc. Moreover, for ions the LET has to be considered, as described above.

DNA damage

The DNA (deoxyribonucleic acid) in the cell nucleus is considered to be the most important target for radiobiological effects. DNA has a double helix structure with two polynucleotide strands held together by hydrogen bonds between the bases of the nucleotides. The double-ringed nucleobases adenine (A) and guanine (G) pair with the single-ringed thymine (T) and cytosine (C), respectively. The double helix interacts with small protein complexes called histones and is arranged in a compact structure called chromatin. The structure of chromatin depends on the stage of the cell cycle: during replication and transcription the chromatin is loosely structured whereas during cell division it is tightly packed.

Radiation may cause damage to the DNA, *e.g.* in the form of breaks on the strands, either directly by ionizing the DNA or indirectly by forming free radicals that damage the DNA. However, DNA damage is not always lethal to the cell. Single strand breaks rarely cause cell death in normal cells since they are easily repaired by the repair system of the cell using the opposite strand as a template. Double strand breaks, breaks close to each other on both of the strands, are more difficult to repair. Cells have two main processes to repair these latter lesions: homologous recombination and non-homologous end joining (Jackson, 2002). In homologous recombination, the sister chromatid or the homologous chromosome is used as a template and the information is copied. In non-homologous end joining the broken strands are simply rejoined and this process is therefore more error-prone. An even more severe damage is multiple strand breaks close to each other, sometimes called clustered DNA damage.

In the repair process, DNA breaks may fail to rejoin correctly and form chromosome aberrations. Serious chromosome changes hinder correct cell division and lead to mitotic death.

High-LET radiation is believed to cause damage that is more difficult to repair compared to low-LET radiation due to the dense ionization pattern which causes multiple strand breaks close in space to a higher degree (Goodhead, 1994; Karlsson and Stenerlöw, 2004). Consequently, the ability of high-LET radiation to cause non-repairable DNA damage is less dependent on alterations such as mutations affecting the cell's repair capacity, cell cycle phase, and environmental conditions such as oxygen pressure.

Cellular response to radiation

One way of measuring the biological effect following irradiation is by the cell survival fraction. The definition of cell survival differs with the context. For proliferating cells, the term clonogenic cell survival is often used and refers to cells that have retained their reproductive capacity *i.e.* cells still capable of undergoing cell division. Cells that are metabolically functioning but not able to divide are not considered survivors with this definition. For most cell types, the dominant mechanism of cell death is mitotic death, *i.e.* death while attempting to divide (Hall and Giaccia, 2006). Another important mechanism for certain cell types is apoptosis, programmed cell death, where the demolition of the cell is more controlled.

A cell survival curve describes the relationship between the absorbed dose and the fraction of cells that survive (see Figure 2). The survival fraction is obtained *in vitro* as the ratio of the plating efficiency of treated cells to that of untreated control cells, where the plating efficiency is the percentage of seeded cells that grow into colonies. Conventionally, the survival fraction is plotted on a log-linear scale with dose on the linear x-axis. The shape of clonogenic cell survival curves as a function of dose is influenced by the type of radiation. For low-LET radiation, the survival curve on a log-linear scale is characterized by a curvature or, as it is commonly called, a shoulder region over the low dose range. For high doses, the curve tends to be more linear, indicating an exponential decrease in cell survival. Historically, two explanations for the curvature have been put forward: interactions of lesions lead to a bend towards lower survival rates; or repair of DNA lesions results in higher survival rates at low to intermediate doses. These theories need not to be mutually exclusive but may be two aspects of the same phenomenon. At low doses the probability of damaging events close to each other may be low giving mostly easily repairable DNA damage, while with increasing dose, the probability of interacting, clustered, damage increases resulting in more severe damage.

Mammalian cells vary considerably in their response to radiation with resistant cell lines showing a large shoulder and sensitive cell lines demonstrating a rapid decrease in the number of colonies formed with increasing dose (Hall and Giaccia, 2006). Cell types prone to apoptotic cell death are more sensitive to radiation than cells dominated by mitotic death, and fast proliferating cells tend to be more sensitive than slowly proliferating cells. Tumor cells generally divide at a high rate and often have malfunctioning cell cycle arrests and repair systems leading to accumulated mutations and damage following irradiation.

In contrast to low-LET radiation, the response following ion radiation shows less dependence on cell type and produces a more straight line in a log-linear sca-

le. Generally, the higher the LET of a radiation the steeper the slope, the more shifted towards lower survival levels, and the smaller the shoulder. An explanation is that high-LET radiation produces more severe damage due to higher probability of damaging events close to each other. However, there is an optimal LET for cell inactivation after which there is a reduced effectiveness in cell inactivation per unit dose with the effect that the slope of the survival curve decrease again. This phenomenon is sometimes called overkill effect.

The biological effectiveness of inducing cell death following ion irradiation is often described in relation to that of photons through the concept of relative biological effectiveness (RBE). The higher the RBE the more effective is the radiation type (see further at page 28).

Organ and tumor response to radiation

Clinical radiation biology often focuses on the relationship between the absorbed dose and resulting response, and on factors influencing this relation. The response in often described as a probability of a specific outcome for the normal tissue or the tumor, typically showing a sigmoid dose-response curve.

Tissues can be classified as serial or parallel, or somewhere in between, based on how their functional subunits are organized. Serial tissues, such as the spinal cord and brain stem, may lose their function even if only a small proportion is severely damaged. Parallel tissues, such as lung and liver, can function even when substantial parts are damaged. Tumors are always assumed to have a parallel function since all clonogenic cells need to be eradicated in order to achieve tumor control.

The response of normal tissues can also be divided into early and late occurring damage, reflecting the time of occurrence of side effects. Rapidly dividing tissues such as skin, bone-marrow, and intestinal epithelium respond early to radiation. Late-responding tissues are for example spinal cord, lung, and kidney.

Dose fractionation

Dose fractionation is the practice of dividing the therapeutic dose into smaller doses delivered over a period of time. It is a key determinant of the therapeutic response. The rational of fractionation is that normal tissues are well-organized and have well-functioning repair systems and may therefore repair radiation-induced damage to some extent between the fractions, whereas tumors are more chaotic in their structure and generally less capable of repair. Another reason is that the fast

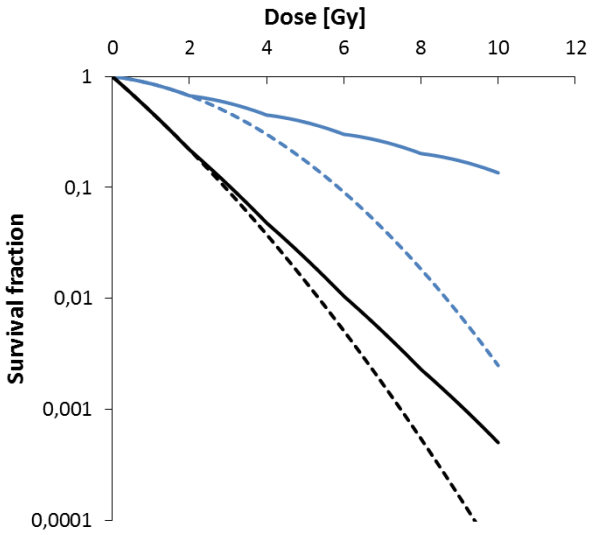

Figure 2: Illustration of cell survival curves obtained following photon irradiation (blue curves) and ion irradiation (black curves). The dashed lines show the survival fraction as a function of single dose, and demonstrate the higher effectiveness of ions over photons. The solid lines illustrate the dose fractionation effect and show the survival fraction after repeated 2 Gy-fractions with complete repair in between.

and poorly organized tumor growth often leads to poor vascular networks resulting in insufficient oxygen levels. Poor oxygenation results in radioresistant cells (Vaupel and Mayer, 2007). After the delivery of dose fractions, the oxygen supply may be improved by hypoxic cells turning oxic due to eradication of the more oxic, radiosensitive, tumor cells or through the reopening of previously closed blood vessels (Toma-Dasu and Dasu, 2013). The main biological processes that affect the fractionation effect are summarized by the five R's of radiobiology:

1. Repair: Repair is one of the primary reasons for fractionation. The smaller dose fractions separated in time allow normal tissue to recover, and normal tissue with intact repair capacity generally has a better ability to repair damage than tumors.

2. Redistribution: Cells in some phases of the cell cycle (M and G2) are more

radiosensitive than in other (S). Dose delivery over time allows for redistribution so that tumor cells in a resistant phase continue to cycle into a more sensitive phase.

3. Reoxygenation: Tumor hypoxia is a condition where tumor cells are deprived of oxygen making them more radioresistant than well oxygenated cells. The oxygenation status may change during treatment and dividing the dose may allow more tumor cells to be eradicated.

4. Repopulation: A prolonged treatment allows normal cells to proliferate which is beneficial. However, also tumor cells proliferate and, especially for fast-growing tumors, a too long treatment time may lead to tumor regrowth.

5. Radiosensitivity: There is also an intrinsic radiosensitivity depending on cell type.

Late-responding tissues are more sensitive to changes in fractionation patterns than early-responding tissues. The difference between these tissues in their response to changes in fractionation could be understood from the differences in their dose-response relations. The cell survival curve for late-responding tissues, with its more curved shape compared to early-responding tissues after photon irradiation, show more sparing when the dose is fractionated. Fewer and larger dose fractions result in more severe late effects even when the total dose is adjusted to produce equal early effects (Hall, 2006). The response following high-LET radiation, with generally straighter cell survival curves, is consequently less affected by fractionation. An illustration of the fractionation effect is shown in Figure 2.

Commonly, around 1.8-2.0 Gy are given per day, five days a week and the treatment takes around 5-7 weeks. For certain tumors, unconventional fractionation schedules have been explored with the hope of increasing the therapeutic ratio. With hyperfractionation, many smaller dose fractions are delivered for example twice a day, whereas in hypofractionation fewer and larger dose fractions are used.

Radiation therapy

Radiation therapy is the use of ionizing radiation for medical treatment, most often of cancer. The ability to ionize atoms and/or molecular structures in the cells, and in that way cause cell death, is utilized. It is given both with the intention to cure the patient and for palliative care, where the aim is to reduce pain or other symptoms. In external beam radiation therapy, which is most commonly used and considered

in this thesis, the patient is exposed to an externally generated beam directed towards the tumor. In internal radiation therapy (brachytherapy), radioactive sources are placed directly at the site of treatment. Some of the advantages of radiation therapy, compared to surgery and chemotherapy, are that it is non-invasive and carries few systemic side effects. Therefore, it may be offered to patients suffering from *e.g.* cardiovascular disease, poor lung function, locally advanced cancer or that are otherwise unfit for surgery; or to patients with *e.g.* dysfunction of the liver, kidney, bone-marrow or otherwise unfit for chemotherapy.

Photon therapy

Photon radiation (x-rays and γ-rays) is the most common modality of radiation. It is widely used and available at most treatment centers. Photons in radiation therapy are typically produced by accelerating electrons in a linear accelerator and colliding them onto a high atomic number target. The resulting high-energetic photons produced are filtered to obtain a uniform intensity field and shaped by a multileaf collimator (MLC). MLC is a beam shaping device consisting of two rows of pairwise opposing leaves of high atomic number material used to create patient-specific field apertures. The accelerator, the beam transport system with bending magnets, and the field-shaping devices are all mounted on a gantry that can rotate around the patient. By rotating the gantry and changing the leaf positions in the MLC, multiple beams from different angles, each shaped as the corresponding tumor projection,

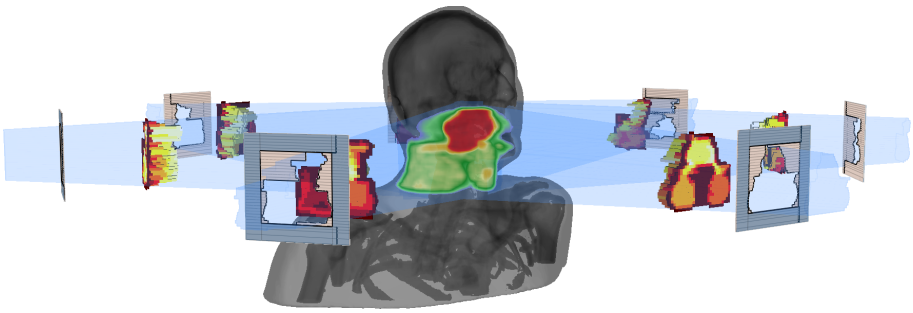

Figure 3: Intensity modulated radiation therapy for a head and neck case. For each beam direction, multiple MLC apertures together yield a fluence modulated field. Combining the fluences from all beam directions together gives the dose distribution in the patient. (Courtesy of Albin Fredriksson and Rasmus Bokrantz.)

give overlapping fields that together conform the tumor volume, a technique called three-dimensional conformal radiation therapy (3DCRT). Thereby a higher dose is delivered to the tumor than to the surrounding normal tissue. In intensity modulated radiation therapy (IMRT), this technique is further improved with the introduction of non-uniform beam fluence profiles. From each beam direction, multiple subsequent apertures together form a field with modulated fluence (see Figure 3). The concept of IMRT was first proposed by Brahme et al. (1982) and Brahme (1988) and is now widely used. This technique yields high conformity in the irradiation of the tumor while avoiding high doses to normal tissue. Instead, larger volumes of normal tissue are typically exposed to low doses compared to 3DCRT, and some concerns about secondary cancer induction in long-term survivors have been raised (Hall, 2006). For reviews of IMRT, see *e.g.* (Ahnesjö et al., 2006; Bortfeld, 2006)

Proton and carbon ion therapy

The main advantages of protons and carbon ions over photons in radiation therapy are: 1) The low dose in the entrance region that slowly increases to near the end of the beam range where a steep increase in dose depositions occur, the Bragg peak, after which the dose sharply drops. This allows for sparing normal tissues surrounding the tumor, and fewer beams are required. 2) The increased biological effectiveness in cell killing at the end of the particle range. The high RBE of carbon ions may be advantageous for radioresitant tumors. Finally, 3) the range of the particles can be controlled by changing their initial energy and thereby the location of the increased dose and effectiveness can be adjusted. However, the range is highly dependent on the stopping power of the traversed medium, which makes protons and carbon ions more sensitive to geometric uncertainties compared to photons. Another disadvantage is the higher cost of setting up the treatment centers.

The beneficial properties of ions can be utilized for improving the probability of local tumor control by delivering higher doses, or for reducing radiation-induced side effects by limiting the dose to normal tissue, or a combination of them. The decreased volume of normal tissue exposed to low doses compared to IMRT may also reduce the risk of radiation-induced secondary cancer. This is particularly important for young patients. Moreover, treatment of radioresitant tumors such as melanoma and sarcomas and hypoxic tumors, which are not efficiently cured by conventional radiation therapy, may benefit from the high RBE of carbon ions. For reviews on radiobiological aspects of ion therapy see *e.g.* (Brahme, 2004; Schulz-Ertner et al., 2006; Jones, 2008; Fokas et al., 2009; Allen et al., 2011).

In ion therapy, a narrow beam is extracted from a particle accelerator. To cover a tumor volume, two main approaches exist: In passive scattering, the beam is broadened laterally by scattering foils and spread out in depth by range modulating devices. The beam can be further shaped laterally by patient-specific apertures and in depth by modulating the distal edge of the beam with patient-specific range compensators. The second technique, pencil beam scanning which is considered in this thesis, the narrow beam is magnetically deflected to scan the beam over the target volume laterally and spread out in depth by changing its energy. A more conform dose distribution to the tumor compared to passive scattering can generally be achieved without patient-specific hardware. More importantly, pencil beam scanning enables intensity modulated proton therapy (IMPT). By varying the time of the pencil beam at each position, the dose distribution can be modulated in three dimensions even from a single beam direction.

Around 35 proton facilities are treating patients today and over 90.000 patients have been treated (PTCOG, 2013). Carbon ions have been used for treatment for a shorter period of time, and six facilities are operating today, three in Japan and one in each of Germany, Italy and China, with over 10.000 patients treated in total (PTCOG, 2013).

Treatment planning

For each patient, an individual treatment plan is made. The patient's internal anatomy is imaged, most often by computed tomography (CT), with the patient immobilized in the position to be used during irradiation. The CT produces cross-sectional x-ray images (or 'slices') that are processed into a three-dimensional (3D) image. Other medical imaging techniques include magnetic resonance (MR) imaging and positron emission tomography (PET).

From the images, the different regions of interest (ROIs) are determined and contoured. The volume including the macroscopic disease, visible from the image, is called the gross tumor volume (GTV). To account for the possible microscopic regional spread of the tumor, a so called clinical target volume (CTV) is contoured, which is an extension of the GTV. The CTV can be further expanded into a planning target volume (PTV) to account for uncertainties arising from *e.g.* patient positioning errors and organ motion. Organs at risk (OAR), *i.e.* organs that may be significantly affected by the radiation, are also contoured. The quantitative physical tissue information obtained from CT images is used also for computing the dose distribution after conversion from Hounsfield units into mass attenuation coefficients.

The treatment planning goals are usually stated in terms of a desired dose distribution. The desired dose to the tumor, generally referred to as the prescribed dose, and the constraints for the irradiation of normal tissue can be stated for example in the following way:

- deliver the prescription dose to at least 95% of the tumor volume
- deliver no less than 95% and no more than 107% of the prescription dose across the tumor volume
- the maximum dose to the ROI may not exceed x Gy
- no more than $v\%$ of the ROI volume may receive x Gy ($D_{v\%} \leq x$)

Dose-volume indices can be represented by a cumulative dose-volume histogram (DVH). The DVH is a cumulative frequency distribution that summarizes a 3D dose distribution in a given volume into a 2D graph. It shows the fraction of the ROI that receives a dose equal to or greater than a given dose level (see Figure 4). Also biological goals can be stated:

- The probability to achieve local tumor control should be at least $p\%$
- The probability to obtain a specified complication should not exceed $p\%$
- The equivalent uniform dose should be x Gy or less

Based on the goals, optimization functions, and possibly constraints, are chosen. Typically, optimization functions penalize deviations from the desired dose criterion in a ROI, and are to be minimized. Several functions can be combined into a single objective function using weights to reflect their relative importance. Biologically-based function can also be optimized such as tumor control probability (TCP) and normal tissue complication probability (NTCP). Numerical optimization techniques are usually used that perform an iterative search through the space of treatment variables to obtain an optimal solution.

The resulting plan needs to be evaluated. The risk of complications (measured directly or indirectly) for each OAR should be acceptably low and the probability of local tumor control should be as high as possible. Often some changes are needed and new optimizations are performed before a satisfying plan is obtained. This iterative manual process of finding a satisfactory trade-off between tumor coverage

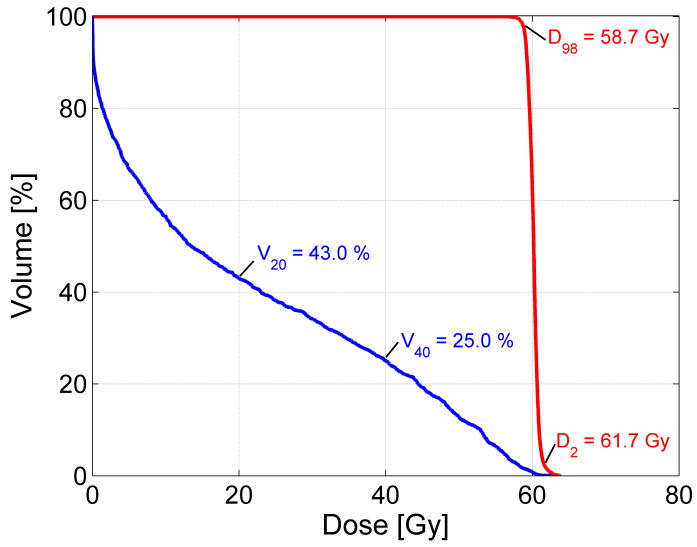

Figure 4: Dose volume histograms and dose volume indices for a tumor volume (red) and an organ (blue). 98% of the tumor volume receive 58.7 Gy or more, and 25% of the organ volume receives 40 Gy or more.

and sparing of different normal tissues can be avoided with multicriteria optimization (Monz et al., 2008; Bokrantz, 2013). Often multiple plans are obtained and compared to determine the best plan.

The difference in planning photon beam therapy and proton and light ion beam therapy stems from differences in physical properties and biological effectiveness (Goitein, 2008). The ability of ions to closely conform the tumor makes them less forgiving if the tumor is somewhat missed. The finite range of ions is strongly affected by the density of the traversed tissue and makes them therefore more sensitive to uncertainties. It is therefore more important to position the patient correctly, and to select 'good' beam directions to avoid beams passing complex inhomogeneities and stopping just before critical structures, if possible. The use of a planning target volume as in photon therapy is less applicable in therapy with intensity modulated charged particles since the PTV generally does not account for the perturbed dose distribution that may arise from changes in densities due to setup errors or organ motion. Optimization methods that account for geometric uncertainties have been developed (Unkelbach et al., 2009; Fredriksson, 2013).

The biological effect of a given dose distribution also differs between photons and ions. For ions, the RBE is used to weight the physical dose to reflect the biological impact. For carbon ions, the RBE can be high and varies considerably across the treatment plan (Kanai et al., 1997; Krämer and Scholz, 2000). Different approaches to account for the RBE of carbon ions are used at different treatment facilities, but they all include a mathematical model for biological effect estimation (Kanai et al., 1997, 1999; Krämer and Scholz, 2000; Combs et al., 2010). For protons, a constant RBE equal to 1.1 is usually assumed in the clinics, although it has been recognized that this assumption is a simplification (ICRU, 2007).

Designing good treatment plans is a complex task. Many factors must be considered and balanced to reach a satisfactory plan. To obtain an optimal treatment plan, it is necessary to know what factors influence the outcome and in what way. Mathematical radiobiological models aim to describe the relation between physical quantities of radiation and biological response.

Aim of the thesis

The aim of this thesis is to develop and evaluate mathematical models for biological effect estimation, with the focus on proton and light ion irradiation. Paper I proposes an extension of the repairable-conditionally repairable damage model to account for the local energy deposition spectrum, as characterized by the LET, for cell survival under light ion irradiation. Paper II proposes a mathematical model to predict the relative biological effectiveness of protons, accounting for cell type, LET, and dose. Paper III evaluates the impact of the RBE variation predicted by the model developed in Paper II in a realistic treatment planning setting, with comparison to the common assumption of a constant RBE equal to 1.1. Paper IV proposes a statistical bootstrap analysis that assesses the uncertainty in clinical outcome data and estimated dose-response relations, due to sampling variability (limited amount of experimental data); the framework is evaluated on photon dose-response data, but is applicable to any model of biological effect estimated from data.

Modeling of radiobiological effects

Mathematical radiobiological models are used for a variety of purposes: to describe the relation between physical quantities of radiation and biological response, to interpolate between known outcomes and to extrapolate beyond what has been studied, to suggest hypotheses to be tested experimentally, to estimate the possible gain of a new treatment strategy, to compare treatment plans, to assist in combining treatment modalities, to re-plan after a non-scheduled treatment interruption, to compensate for earlier delivered over- or underdosage, generally to assist in decision-making, and more. It is not possible to experimentally test all combinations of irradiation conditions of interest. With mathematical models, what-if analyses are easily made to explore the impact of changes in the input assumptions. Radiobiological models are also used to convert the absorbed dose to clinically more relevant quantities such as biologically equivalent dose, tumor control probability and normal tissue complication probability. In ion radiation therapy, radiobiological models are used to estimate the relative biological effectiveness.

Cell survival models

A cell survival curve describes the relationship between the absorbed dose and the fraction of surviving cells. Cell survival models aim to describe this curve, and form the basis for many dose-response models. The latter describe the probability of a specific biological response at a given dose. Three cell survival models are described here: the linear, the linear-quadratic (LQ), and the repairable-conditionally repairable damage (RCR) model. The linear model is the simplest, the LQ model is the most widely used, and the RCR model is a newly developed model with some advantageous properties. Other models include those described by Tobias (1985);

Curtis (1986) and Sontag (1997) and models based on target theory first described by Lea (1946).

The linear cell survival model

The clonogenic cell survival as a function of dose is in a first approximation an exponential process. In the simple linear cell survival model it is assumed that a single "hit" or "damaging event" on a critical target in the cell leads to cell death. The expression for expected survival fraction is

$$S_L(D) = \frac{N(D)}{N_0} = e^{-\frac{D}{D_0}} \tag{2}$$

where $N(D)$ denotes the number of cells surviving a dose D, N_0 is the initial number of cells, and D_0 is the dose giving one hit per target on average, which reduces the survival fraction by a factor 0.37 (e^{-1}). The model is also called the single-hit single-target model.

The linear-quadratic cell survival model

The fraction of surviving cells as a function of dose is usually not an entirely exponential process as assumed by the linear cell survival model, but exhibits a curvature. The linear-quadratic (LQ) model (Lea and Catcheside, 1942; Sinclair, 1966; Kellerer and Rossi, 1978; Chadwick and Leenhouts, 1973; Barendsen, 1982) can handle this type of response. This is a well-established and widely used model. For a single dose (one dose fraction) the model is expressed as:

$$S_{LQ}(d) = e^{-\alpha d - \beta d^2} \tag{3}$$

where α and β are the parameters of the model. α is associated with the initial slope and β with the curvature. The α/β ratio describes the fractionation sensitivity of a tissue and the inherent sensitivity of a cell type. As a general rule of thumb, late-responding tissues have low α/β values (around 3 Gy) while early-responding normal tissue and most tumors have a larger α/β value (around 10 Gy). There are exceptions such as prostate tumors with biological properties more like those of slowly proliferating late-responding tissues (Brenner and Hall, 1999) and exhibit a low α/β ratio around 1.5 Gy (Dasu and Toma-Dasu, 2012; Fowler et al., 2013). A small α/β value indicates that large fractional doses are not well tolerated.

The total survival fraction after n dose fractions is obtained as

$$\begin{aligned} S_{LQ}(D) &= \prod_{k=1}^{n} S_{LQ}(d_k) = \prod_{k=1}^{n} e^{-\alpha d_k - \beta d_k^2} \\ &= \exp\left(\sum_{k=1}^{n} \left(-\alpha d_k - \beta d_k^2\right)\right) \\ &= \exp\left(\sum_{k=1}^{n} -\alpha d_k \left(1 + \frac{d_k}{\alpha/\beta}\right)\right) \end{aligned} \tag{4}$$

where D denotes the total dose, and d_k is the dose of the kth fraction. When the fractional doses are equal this expression simplifies to

$$S_{LQ}(D) = (S_{LQ}(d))^n = e^{-\alpha n d - \beta n d^2} = e^{-\alpha D(1+\frac{d}{\alpha/\beta})}. \tag{5}$$

In its simplest form, it is assumed that full repair of sub-lethal damage occurs between each dose fraction, and that no repopulation occurs. The LQ model can be reformulated to account for incomplete repair due to dose fractions close in time, and to account for the effect that cells may start to divide at a higher rate after some time following irradiation (Dale and Jones, 2007). Furthermore, the inducible repair model (Joiner and Johns, 1988) is a modified LQ model to handle low-dose hypersensitivity, the phenomenon observed experimentally of high radiation sensitivity to doses below around 0.5 Gy (Joiner et al., 2001).

A drawback with this model is the constant curvature which is not consistent with experimental observations which indicate that the survival curve becomes more or less linear (in a log-linear scale) at high doses. The model is therefore modified in the local effect model (LEM), where the LQ model is a part, used clinically in the carbon ion treatment in Heidelberg (Scholz et al., 1997; Elsässer and Scholz, 2007; Elsässer et al., 2008, 2010). In LEM, the curve is simply extrapolated by a straight line at doses higher than at threshold dose d_t:

$$S_{LQ'}(d) = \begin{cases} e^{-\alpha d - \beta d^2} & \text{if } d \leq d_t \\ e^{-\alpha d - \beta d^2 - (\alpha + 2\beta)(d - d_t)} & \text{if } d > d_t \end{cases} \tag{6}$$

The LQ model may also be inappropriate for treatments with high doses per fractions used in stereotactic radiation therapy and in hypofractionation (Kirkpatrick et al., 2009), and for ions showing a cell survival curve with a small shoulder that transform into an exponential curve already at low doses.

The repairable- conditionally repairable damage model

The repairable- conditionally repairable damage (RCR) model (Lind et al., 2003) is a radiobiological model that can describe cell survival for a wide range of doses accounting for low-dose hypersensitivity, the shoulder region, and a quasi-linear survival curve for high doses. It separates the probability of inducing damage and the probability of cellular repair, enabling studies of these effects individually. The RCR model assumes that a cell can survive either by not receiving any damage or by correctly repairing the acquired damage. The cell survival fraction as a function of dose is approximated by

$$S_{RCR}(D) = e^{-aD} + bDe^{-cD} \tag{7}$$

where D denotes the dose, and a, b, and c are the parameters of the model. The first term, $\exp(-aD)$, represents the fraction of cells not being damaged, and the second term, $bD\exp(-cD)$, is the fraction of cells that have been damaged and subsequently repaired.

In Paper I, we extended the RCR model with a parameterization by LET to provide a radiobiological model for ions that accounts for both dose and LET. The LET dependence was incorporated in the RCR model by expressing its parameters a, b, and c as functions of LET (L) instead of free parameters. In that way, the model can directly estimate the survival fraction for any dose and LET combination. The survival fraction expressed with the LET-parameterized RCR model is

$$S_{RCR}(D) = e^{-a(L)D} + b(L)De^{-c(L)D} \tag{8}$$

where

$$\begin{aligned} a(L) &= a_0 e^{-\left(\frac{L}{L_a}\right)^2} \\ b(L) &= b_0 e^{-\frac{L}{L_b}} \\ c(L) &= \frac{c_0}{L/L_c}\left(1 - e^{-\frac{L}{L_c}}\left(1 + \frac{L}{L_c}\right)\right) \end{aligned} \tag{9}$$

With these expressions, the fraction of damaged cells as a function of LET,

$$f_{\text{damage}}(L) = 1 - e^{-a(L)D}, \tag{10}$$

decreases rapidly at high LETs for a constant dose level due to damage clustering, and the normalized fraction of repaired cell,

$$f_{\text{repair}}(L) = \frac{b(L)De^{-c(L)D}}{1 - e^{-a(L)D}}, \tag{11}$$

shows a decrease already at low LETs.

The model predicts a cell survival curve with negative slope that increases with increasing LET and exhibits a shoulder that decreases with increasing LET. Moreover, it handles the reduced effectiveness in cell inactivation for LETs higher than the optimal LET giving decreasing slopes again but still with no or greatly reduced shoulders. This overkill effect could be explained by a trade-off between the severity and number of lethal events so that even more severe damage in fewer sites becomes less effective.

By expressing the parameters as functions of LET instead of as free parameters, and by fitting the cell survival curves of all LETs simultaneously instead of for each LET, a somewhat less accurate fit to the experimental data for a given cell line is obtained. The benefits include the possibility to estimate cell survival also for dose and LET combinations for which we have no experimental data available, and the reduced risk of overfitting to available experimental data.

Tumor control and normal tissue complication probability models

In clinical radiation biology, the response of a biological system following irradiation is often expressed as a probability of response. The normal tissue complication probability (NTCP) and the tumor control probability (TCP) depend on a large number of factors. Here we consider mainly dose and volume effects.

Dose-response models

A dose-response model describes the response probability as a function of dose. Usually a sigmoid relation is assumed, most often characterized by its position and the steepness of its slope. The position of the curve is usually quantified by the dose required to obtain a certain probability of response such as 37% (D_{37}) or 50% (D_{50}). The often preferred description of the slope is the so called normalized dose-response gradient where the dose-response gradient is steepest, γ (Brahme, 1984). It describes the change in response probability for a given relative increase in absorbed dose.

Poisson distribution based models

Assume that there are N_0 clonogenic tumor cells or functional subunits to begin with, all with the same probability of survival at a given dose, $S(D)$, and that the

survival of each cell is independent of the survival of other cells. Then the number of surviving cells X follows the binomial distribution $X \sim \text{Bin}(N_0, S(D))$.

The typical tumor contains a large number of clonogenic tumor cells, and effective irradiation requires that the probability of survival for each individual cell is low. Under such circumstances, the Poisson distribution is a good approximation of the binomial distribution. The Poisson distribution is a discrete probability distribution for random variables that denotes the number of discrete events in a given interval. The probability mass function of a discrete stochastic variable X that follows a Poisson distribution is given by

$$P(X = k \mid \lambda) = \frac{\lambda^k e^{-\lambda}}{k!} \tag{12}$$

where k is the actual number of events and λ is the expected value.

In radiation therapy one important issue is how much dose is required to inactivate the tumor, and it is usually assumed that all clonogenic tumor cells have to be eradicated to control the tumor. In other words, the model seeks to estimate the probability to eradicate all tumor cells (k = 0) given that the expected number of surviving cells λ depends on the dose. The expected number of surviving cells can be estimated from the initial number of cells N_0 and the fraction of surviving cells (probability of survival of each cell) S. From this, the probability of no surviving cells can be expressed as

$$P(X = 0 \mid D) = e^{-\lambda(D)} = e^{-N_0 S(D)}. \tag{13}$$

The fraction of surviving cells can be obtained from a cell survival model, such as the linear cell survival model (2), the LQ model (5) or the RCR model (7). Using the linear cell survival model we obtain the following expression for the probability of response as a function of dose

$$P_L(X = 0 \mid D) = e^{-N_0 S_L(D)} = e^{-N_0 \exp\left(-\frac{D}{D_0}\right)} \tag{14}$$

This model can be expressed also by the clinically important parameters D_{50} and γ. Via the definition of γ (Brahme, 1984), the following relation with the initial number of cells is obtained:

$$\gamma \equiv D\text{max}\frac{dP}{dD} = \frac{\ln N_0}{e}. \tag{15}$$

By inserting the dose giving a 0.5 probability for the response (D_{50}) we obtain

$$D_{50} = D_0 \left(e\gamma - \ln\left(\ln 2\right)\right). \tag{16}$$

The linear dose-response model can thus be expressed as

$$P_L(X = 0 \mid D) = e^{-\exp\left(e\gamma - \frac{D}{D_{50}}(e\gamma - \ln(\ln 2))\right)}. \tag{17}$$

If instead the dose-response model is based on the LQ model, the following expression is obtained:

$$\begin{aligned} P_{LQ}(X = 0 \mid D) = e^{-N_0 S_{LQ}(D)} = e^{-N_0 \exp\left(-\alpha D\left(1 + \frac{d}{\alpha/\beta}\right)\right)} = \\ = e^{-\exp\left(e\gamma - \alpha D\left(1 + \frac{d}{\alpha/\beta}\right)\right)} \end{aligned} \tag{18}$$

The parameter D_{50} can be included in the LQ model by assuming $P_{LQ}(D)$ = $P_L(D)$ for a given fractional dose d_{ref} for which D_{50} and γ were determined, usually 2 Gy, which gives (Lind et al., 1999):

$$\alpha = \frac{e\gamma - \ln(\ln 2)}{D_{50}\left(1 + \frac{d_{\text{ref}}}{\alpha/\beta}\right)} \tag{19}$$

Using this expression for the parameter α, the LQ dose-response model, $P_{LQ}(D)$, is equivalent to the linear dose-response model using the equivalent dose (EQD, see page 27) $P_L(EQD)$.

In practice, γ and D_{50} are not derived from (15) and (16), but treated as free parameters and estimated with for example maximum likelihood to achieve the best possible fit to the dose-response data at hand. In a similar fashion, the models described above can be fitted to experimental data for normal tissue complication, as in Paper IV for the dose-response relations of myelopathy (spinal cord) and pneumonitis (lung).

Normal distribution based model

The Lyman model (Lyman, 1985) is based on the cumulative distribution function of the normal distribution:

$$P_{Lyman}(D) = \frac{1}{\sqrt{2\pi}} \int_{-\infty}^{t} e^{\frac{-x^2}{2}} \mathrm{d}x = \frac{1}{2}\left(1 - \operatorname{erf}\left(\frac{t}{\sqrt{2}}\right)\right) \tag{20}$$

with the upper limit t defined as

$$t = \frac{D - D_{50}}{mD_{50}}$$

where m denotes the slope.

Paper IV compared the Lyman model (20) and the Poisson-based linear dose-response model (17) in terms of estimated parameters and the fit to clinical outcome data.

Dose-volume response models

Different parts of an organ and, to a lesser extent, a tumor may be irradiated with different doses. The probability of a given response depends on the distribution of the dose within each volume. Organs also exhibit complex functional relations between different compartments which means that the function of an organ may be dependent of how large fraction of it has been irradiated. In this context the publication by Withers et al. (1988) has been important where they assume that normal tissue behavior depends on its architecture, stated as being serial or parallel, as described above. In a completely serial tissue, the inactivation of one functional subunit is sufficient to cause the endpoint considered. For such tissues the probability of response is largely determined by the maximum dose. A parallel tissue may preserve its function as long as a critical fraction of its volume is functioning. For this type of tissue, the mean dose is an important measure for determining the outcome probability.

In treatment planning, the patient geometry is discretized into small volume elements called voxels. In calculating the response one assumes that these volumes are small enough so that the dose is uniform within each one. All voxels are usually assumed to have the same radiosensitivity so that they respond with the same probability to a specific dose. It is of course possible to designate a different radiosensitivity to for example a known hypoxic region within a tumor. Different voxels are also considered independent. However, there have been observations that cells communicate by intercellular signaling so that the response of cells do depend on other cells, the so-called bystander effect (Prise and O'Sullivan, 2009).

The tumor control probability denotes the probability that the number of clonogenic tumor cells capable of cell division is zero after the last dose fraction. The TCP can be formulated as the product of the probabilities of cell death of all voxels M as:

$$TCP(D) = \prod_{i=1}^{M} (P(D_i)) \tag{21}$$

where D_i is the total dose to voxel i. A Poisson-based (13) or a binomial-based dose-response expression can for example be used for $P(D_i)$. If a single voxel receives no dose there is no change of eradicating all tumor cells in that voxel, and the model predicts zero probability of tumor control. The minimum dose has a major impact on the TCP and cold spots should be avoided.

The relative seriality model developed by Källman et al. (1992) handles normal tissue that has mixed serial and parallel behavior. The model uses the "relative seriality" parameter s to describe the volume effect. This parameter s ranges from low values for parallel types of tissue to high values for serial tissue. The NTCP is expressed as

$$NTCP_s(D) = \left(1 - \prod_{i=1}^{M} (1 - P(D_i)^s)^{\frac{v_i}{V_{\text{ref}}}}\right)^{1/s} \tag{22}$$

where v_i/V_{ref} is the relative volume of voxel i compared to the reference volume.

Paper III used this model, with the probability of response $P(D_i)$ calculated with the Poisson-based linear-quadratic model (18), to estimate NTCP following proton and photon irradiation in treatment plan comparison.

Another common NTCP model is the Lyman Kutcher Burman (LKB) model (Lyman, 1985; Kutcher and Burman, 1989). This model is the Lyman model (20) extended with a volume effect. The upper limit t of the integral in the cumulative normal distribution is here instead expressed as

$$t = \frac{D - D_{50}(v/V_{\text{ref}})}{mD_{50}(v/V_{\text{ref}})} \tag{23}$$

where

$$D_{50}(v/V_{\text{ref}}) = D_{50}(1)\left(\frac{v}{V_{\text{ref}}}\right)^{-n}$$

$D_{50}(1)$ denotes the dose giving 50% complication probability for uniform irradiation of the whole organ and v/V_{ref} is the volume fraction. n specifies the volume dependence.

Other models include the critical-element model (Niemierko and Gotein 1991), critical volume model (Niemierko and Gotein 1993), parallel architecture model (Jackson 1995), and Weibul distribution model (Klepper 2001).

Individual TCPs and NTCPs can be combined into composite probabilities. The probability of complication-free tumor control, $P+$, is an attempt to combine probabilities into a single measure of the overall quality of the treatment plan (Lind et al., 1999):

$$P_+(D) = TCP(D)\,(1 + NTCP(D)) \tag{24}$$

Which NTCPs to be included into the $P+$ expression is essential. Failure to control the tumor should not be balanced against the risk of minor normal tissue complications. Only the NTCP of severe complications should be considered to be included in the calculation of $P+$.

Biologically equivalent doses

The vast majority of treatments with radiation therapy to date are performed using photon beams. For decades, uniform intensity beams were used, fraction doses around 2 Gy have been given, and treatment goals stated in terms of dose. To take advantage of the vast experience gained from conventional radiation therapy, non-standard photon doses and ion doses are converted to traditional photon doses (rather than to biological outcome). The underlying assumption is that different doses are equivalent if they cause the same biological effect. Another benefit of the expressions of biologically equivalent doses is that they allow for direct comparison of different treatment plans.

Equivalent uniform dose

The concept of the equivalent uniform dose (EUD) was proposed by Niemierko (1997). The idea is that any dose distribution has a corresponding uniform dose that causes an equivalent biological response. Originally EUD was defined for tumors only and was based on survival fractions, but was later refined (Niemierko, 1999) to apply also for normal tissues, in what is referred to as the generalized EUD:

$$EUD = \left(\sum_{i=1}^{M} v_i d_i^a \right)^{1/a} \tag{25}$$

where d_i denotes the dose in voxel i, v_i is the fraction of the volume of interest that is occupied by voxel i, M is the total number of voxels, and a ($\neq 0$) is a tissue specific parameter that controls the volume effect. As $a \to \infty$, EUD approaches its maximum. For tissues where the biological effect is highly dependent on maximum doses, *i.e.* serial tissues, a large positive a value is used so that larger doses are given higher weight. As a = 1, EUD becomes the arithmetic mean dose, and therefore parallel-structured organs have an a value close to unity. For tumors, negative values are used so that cold spots have a large effect on the EUD.

Equivalent dose in 2 Gy fractions

The standard fractionation schedule of around 2 Gy per day for five days a week is probably not optimal for all cases. EQD_2, the equivalent dose in 2 Gy-fractions, is used for example to compare fractionation schedules. It estimates the total dose delivered in 2 Gy-fractions that would yield the same biological effect as the total dose obtained using the fractionation schedule of interest. A general expression for EQD can be derived from the LQ cell survival model (Eq. 4):

$$S_{LQ}(D) = e^{\left(\sum_{k=1}^{n} -\alpha d_k \left(1+\frac{d_k}{\alpha/\beta}\right)\right)} = e^{-\alpha D_{\text{ref}}(1+\frac{d_{\text{ref}}}{\alpha/\beta})} = S_{LQ}(D_{\text{ref}}) \tag{26}$$

where n is the total number of fractions. D_{ref} is here the reference total dose that give the equivalent effect, *i.e.*, the EQD:

$$EQD = \frac{\sum_{k=1}^{n} d_k \left(1+\frac{d_k}{\alpha/\beta}\right)}{1+\frac{d_{\text{ref}}}{\alpha/\beta}} \tag{27}$$

where d_{ref} denotes the reference fraction dose. If equal fraction doses d_k are used and d_{ref} = 2 Gy, this expression reduces to

$$EQD_2 = \frac{D\left(1+\frac{d}{\alpha/\beta}\right)}{1+\frac{2}{\alpha/\beta}}. \tag{28}$$

If two treatment plans with different fractionation schedules are to be compared and both are rescaled using EQD_2, the treatment plan with the highest EQD_2 will give more damage than the other plan, according to the model.

A closely related concept also used is the biologically effective dose (BED) (Barendsen, 1982; Dale, 1985; Jones et al., 2001; Fowler, 2010). The BED is defined as

$$BED = \frac{-\ln S_{LQ}}{\alpha} = D\left[1+\frac{d}{\alpha/\beta}\right] \tag{29}$$

where the expression in the brackets is the relative effectiveness (RE). By dividing the BED with the RE of a reference radiation schedule, EQD is obtained.

Just as incomplete repair and repopulation can be incorporated into the LQ model, these effects can also be accounted for in EQD and BED.

Relative biological effectiveness

Relative biological effectiveness is defined as the ratio of the dose of a reference radiation, normally low-LET photons, and the corresponding ion dose giving the same biological response under otherwise equal conditions:

$$RBE = \frac{D_{\text{ref}}}{D}. \tag{30}$$

It is a measure of the efficiency of producing a specific response by a radiation type and provides a link between the dose of ions and the dose of photons. The physical ion dose can be multiplied with the RBE to obtain a photon equivalent dose with the unit Gy(RBE). It is essential that an appropriate RBE value is used since an incorrect RBE value may propagate into inappropriately chosen ion prescription doses, give a higher biological effect in normal tissues than intended, and hinder correct plan comparison. RBE-models aim at estimating this relative biological effectiveness.

The biological efficiency is generally higher for ions, but the efficiency has been found to depend on various factors (Gerweck and Kozin, 1999; Kraft, 2000; Weyrather and Debus, 2003). Since the RBE is defined relative to sparsely ionizing radiation that often shows a non-linear response to dose, RBE depends on the dose level. RBE increases with decreasing dose per fraction.

Another clear trend is that RBE varies with LET. With increasing LET the damage becomes more severe and more difficult to repair resulting in higher radiation lethality, and reflected by a higher RBE. However, there is a maximum after which the effectiveness is reduced and RBE decreases. The RBE maximum appears at LET values around 30 keV/μm for protons (Belli et al., 1998), but is shifted to greater LET values for heavier ions (Kraft, 2000). Thus, the biological effect varies between ions at the same dose and LET. This is a result of differences of the distribution of ionizing events. Also the maximum RBE that can be obtained differs between ions, with the higher LETs of carbon ions compared to protons translating into higher maximum RBE.

Moreover, RBE varies between different cell and tissue types. Slowly proliferating cells tend to yield larger RBE than fast proliferating cells, and cells with a

high repair capacity give larger RBE than poorly repairing cells. RBE also varies across endpoints.

In proton radiation therapy, the majority of therapy centers assume a constant RBE value of 1.1 for all clinical situations regardless of the physical properties of the proton beams and the biological system. The LET variation is relatively small and therefore a constant RBE has been considered as an acceptable simplification. For carbon ions, the RBE is higher and the variation is larger and, therefore, no single RBE value is appropriate for every combination of factors affecting the RBE.

A general RBE-expression can be derived based on the LQ model (5) together with the definition of RBE:

$$S = e^{-\alpha d - \beta d^2} = e^{-\alpha_{\text{phot}} d_{\text{phot}} - \beta_{\text{phot}} d_{\text{phot}}^2} = S_{\text{phot}} \tag{31}$$

where d is the fraction dose, and all quantities with the subscript phot refer to photon radiation while the others refer to ion radiation. By solving a second-degree equation for the positive root, one obtains

$$d_{\text{phot}} = -\frac{1}{2}\left(\frac{\alpha}{\beta}\right)_{\text{phot}} + \sqrt{\frac{1}{4}\left(\frac{\alpha}{\beta}\right)_{\text{phot}}^2 + \frac{\alpha}{\beta_{\text{phot}}} d + \frac{\beta}{\beta_{\text{phot}}} d^2} \tag{32}$$

The RBE at a certain ion dose d can then be expressed as

$$\begin{aligned} RBE(d) &= \frac{d_{\text{phot}}}{d} = \\ &= -\frac{1}{2d}\left(\frac{\alpha}{\beta}\right)_{\text{phot}} + \frac{1}{d}\sqrt{\frac{1}{4}\left(\frac{\alpha}{\beta}\right)_{\text{phot}}^2 + \frac{\alpha}{\alpha_{\text{phot}}}\left(\frac{\alpha}{\beta}\right)_{\text{phot}} d + \frac{\beta}{\beta_{\text{phot}}} d^2} \end{aligned} \tag{33}$$

In paper II, we developed an RBE model specifically for protons based on this expression. A parameterization by LET and cell type was incorporated. The approach was to study the proton parameters α and β by investigating how $\alpha/\alpha_{\text{phot}}$ and $\beta/\beta_{\text{phot}}$ varies with LET, for a set of experimental data. We then investigated how this LET-dependence is affected by cell type as characterized by $(\alpha/\beta)_{\text{phot}}$.

Based on experimental $in\ vitro$ data of a range of different cell types irradiated with protons of well-defined dose and LET, the $\alpha/\alpha_{\text{phot}}$ was found to increase with increasing LET with a slope inversely depending on cell type. However, no statistically significant relation between $\beta/\beta_{\text{phot}}$ and LET was found and β for protons was assumed to be equal to that of photons. The resulting RBE expression

describes the RBE as a function of dose, LET, and $(\alpha/\beta)_{\text{phot}}$:

$$RBE\left(d, LET, (\alpha/\beta)_{\text{phot}}\right) = -\frac{1}{2d}\left(\frac{\alpha}{\beta}\right)_{\text{phot}} + \\ + \frac{1}{d}\sqrt{\frac{1}{4}\left(\frac{\alpha}{\beta}\right)^2_{\text{phot}} + \left(0.434LET + \left(\frac{\alpha}{\beta}\right)_{\text{phot}}\right)d + d^2} \tag{34}$$

The model predicts a tissue-dependent relation between RBE and LET determined by the $(\alpha/\beta)_{\text{phot}}$ ratio: the RBE increases with increasing LET for cell lines with low $(\alpha/\beta)_{\text{phot}}$ ratio, but the relation becomes weaker with increasing $(\alpha/\beta)_{\text{phot}}$, and at high $(\alpha/\beta)_{\text{phot}}$ ratios, RBE is low and insensitive to LET changes. Moreover, the model shows an increasing RBE with decreasing dose per fraction and the effect is most pronounced for low $(\alpha/\beta)_{\text{phot}}$ values.

This RBE model does not account for the decrease in RBE that occurs at LETs higher than around 30 keV/μm. However, in clinical proton therapy that high LET values are of little practical relevance.

Other RBE models include (Hawkins, 1998; Dale and Jones, 1999; Wilkens and Oelfke, 2004; Tilly et al., 2005; Carabe et al., 2012; Frese et al., 2012).

Model selection and evaluation

Models are approximations of reality, and their predictions are subject to uncertainty. Even when the input, such as absorbed dose and LET, is accurately described, the output, such as survival fraction or NTCP, can have large uncertainties. Living systems are complex, with individual heterogeneity, interactions, and environmental covariates, and radiobiological models can at best give good approximations. However, the uncertainty in the output is not only due to limitations in how accurately the model captures reality but also to uncertainties in its parameters, which are estimated from limited empirical data. As George E. P. Box put it (Box and Draper, 1987): "All models are wrong, but some are useful". To judge if a model is useful it needs to be evaluated, and if there are a number of candidate models, methods are needed to select the most useful one.

Parameter estimation

Once a model is specified, the parameters that give the best fit of that model to data can be assessed through parameter estimation. Two well-known methods are least squares estimation (LSE) and maximum likelihood estimation (MLE).

The method of least squares estimation is a standard approach in many natural sciences and is linked to concepts such as root mean squared deviation, and coefficient of determination (r2). The best estimates of the parameters θ to data y given a model f are those that minimizes the sum of squared error (SSE) - hence the name of the method. Error here denotes the difference between the predicted and observed value at each data point.

$$\text{SSE}(\theta) = \sum_i \left(y_i - f(x_i, \theta)\right)^2 \tag{35}$$

LSE makes no explicit assumptions of the probability distribution of observed quantities.

Maximum likelihood estimation is based on the probability density function $f(y \mid \theta)$ that specifies the probability of observing the data y given the parameter vector θ. The likelihood takes the inverse perspective: what is the likelihood of the parameter θ given the observed data, $\mathcal{L}(\theta \mid y) = f(y \mid \theta)$. That is, under the assumption of a given model, what parameter values yield the highest probability for the observed data. In MLE the attempt is to find the parameter values that make the observed data "most likely", *i.e.*, that maximizes the likelihood function $\mathcal{L}(\theta \mid y)$. If individual data points y_i are independent of each other, the likelihood function can be expressed as

$$\mathcal{L}(\theta \mid y) = \prod_i f(y_i \mid \theta) \tag{36}$$

Maximizing the product is equivalent to maximizing the logarithm of the likelihood

$$\ln\mathcal{L}(\theta \mid y) = \sum_i \ln f(y_i \mid \theta) \tag{37}$$

Many model selection criteria such as the Akaike information criterion (AIC) (Akaike, 1973), Baysian information criterion (BIC) (Schwarz, 1978), and Vuong's test (Vuong, 1989) are based on MLE.

In Paper IV, MLE was used to fit two dose-response models, a Poisson-based linear model (17) and the Lyman model (20), to clinical outcome data. For each study setting i, the outcome data was presented as the proportion of patients in which the studied endpoint was detected giving a binomially distributed outcome. The likelihood function was therefore expressed as

$$\mathcal{L}(\theta \mid N, cases) = \prod_i P(D_i, \theta)^{cases_i} \left(1 - P(D_i, \theta)\right)^{N_i - cases_i} \tag{38}$$

where $P(D, \theta)$ denotes the probability of the adverse event at a given dose predicted either by the Poisson-based linear model or the Lyman model, N denotes the total number patients in the study, and $cases$ denotes the number of occurrences of the studied endpoint.

If the observations are independent and normally distributed with a constant variance, LSE and MLE result in the same parameter estimates. Otherwise, different conclusions of the same observed data can be made depending on the method used.

Statistical hypothesis testing

Statistical hypothesis tests attempt to reject hypotheses based on observed data. The research question is expressed as a null hypothesis, which states the opposite of what we seek to show. The goal is to investigate if there is sufficient evidence to reject the null hypothesis in favor of the alternative hypothesis. A statistically significant result is one assessed as unlikely to have occurred by chance under the null hypothesis. A threshold probability, called the significance level, is predefined to determine how unlikely an observed result must be in order to be classified as statistically significant.

The development of the RBE model for protons in Paper II was driven largely by hypothesis tests. The significance level was consistently set to 0.05, and the data consisted of experimentally obtained LQ parameter values from a range of different cell lines irradiated with protons, and with photons as a reference. Our first aim was to explore whether there exists a linear dependence between $\alpha/\alpha_{\text{phot}}$ and LET

$$f(LET) = \frac{\alpha}{\alpha_{\text{phot}}}(LET) = 1 + k \cdot LET + \epsilon \tag{39}$$

where ϵ is assumed to be independent and normally distributed random errors. The null hypothesis was that k equals zero. The test statistic for the slope of a linear regression model is:

$$t_k = \frac{k - k_0}{\text{SE}(k)} \tag{40}$$

which follows a t_{n-2} distribution if the null hypothesis is true. k is the estimated slope based on the observations in the sample and k_0 is the slope of the null hypothesis. SE(k) denotes the standard error of the slope and can be computed as

$$\text{SE}(k) = \frac{\sqrt{\frac{1}{n-2}\sum_{i=1}^{n}\left(y_i - f(LET_i)\right)^2}}{\sqrt{\sum_{i=1}^{n}\left(LET_i - \overline{LET}\right)^2}} \tag{41}$$

where y denotes the experimentally obtained $\alpha/\alpha_{\text{phot}}$ values, $\overline{LET}$ is the mean LET, and n is the number of data points. If the test statistic t_k is large *i.e.* if the estimated slope is large compared to its standard error, then the null hypothesis is rejected. We used the one-tailed t-test since we are interested in the hypothesis that the slope $k > 0$, and obtained a p-value < 0.05 allowing us to conclude that the slope

is statistically significantly greater than zero at this significance level, meaning that there is a positive relation between $\alpha/\alpha_{\text{phot}}$ and LET.

The same procedure was performed to test if there exists a linear dependence between $\beta/\beta_{\text{phot}}$ and LET. Here, the null hypothesis could not be rejected. In other words, we did not find statistical support to include such a relation in our model.

In case of the intercept, it is often assumed to be 1 since the biological effectiveness of protons is assumed to approach that of photons as LET decreases. There is no natural null hypothesis to test this assumption, so instead we constructed a 95% two-sided confidence interval for the intercept:

$$m \pm t_m \cdot \text{SE}(m) \tag{42}$$

where the standard error of the intercept is expressed as

$$\text{SE}(m) = \sqrt{\frac{1}{n-2}\sum_{i=1}^{n}\left(y_i - f(LET_i)\right)^2} \cdot \sqrt{\frac{1}{n} + \frac{\overline{LET}^2}{\sum_{i=1}^{n}\left(LET_i - \overline{LET}\right)^2}} \tag{43}$$

The confidence interval included our assumed value of 1.

Model selection

Akaike information criterion

The Akaike information criterion (AIC) (Akaike, 1973) is a measure used for selecting the best fitting model from a set of possible models. The models do not need to be nested. AIC gives a relative estimate of the information lost when a given model is used to approximate the "true model", that is, the unknown model that generated the data of interest. Thus, the model that is closest to the true model, based on the expected Kullback-Leibler distance, is the one that minimizes the information loss (Burnham and Anderson, 2002). The AIC is computed as

$$AIC = -2\ln\mathcal{L} + 2K \tag{44}$$

where $\mathcal{L}$ is the maximum likelihood estimate and K is the number of parameters in the model. An AIC is computed for each candidate model and the preferred model is the one with the lowest AIC value. Generally, the likelihood may be increased by increasing the number of parameters, but the $2K$ term in the expression is effectively a penalty for extra parameters. Thus, this model selection technique balances goodness of fit with model complexity.

AIC selects the best model in the set of models considered. However, it does not state if one model is significantly better than another or the quality of fit for any of them.

Bayesian information criterion

The Bayesian information criterion (BIC) (Schwarz, 1978) is an alternative model selection criterion. It is derived in a Bayesian setting and favors the model with highest probability given the observed data. The form of BIC is closely related to that of the AIC but with different penalty for model complexity

$$BIC = -2\ln\mathcal{L} + K\ln n \tag{45}$$

where n is the number of data points. In practice, BIC imposes a stronger penalty for complexity. One advantage of BIC over AIC is that the probability of it selecting the true model (if part of the considered set of models) approaches 1 as sample size approaches infinity. The same is not true for AIC. On the other hand, in finite samples BIC tend to choose too simple models (Hastie et al., 2009).

Vuong's statistical test

Vuong's statistical test (Vuong, 1989) is a likelihood ratio-based test for model selection that can be used for non-nested models. The null hypothesis is that the two models compared are equally close to the "true" model, whereas the alternative hypothesis is that one model is closer, where the "closeness" is determined by the expected Kullback-Leibler distance. Hence, the test not only ranks which model is the most likely to generate the given data, but also determines if one model is significantly better than another. Unlike for example AIC and BIC, it may conclude that data does not strongly support one model over the other.

In Paper II, Vuong's test was used to evaluate if the LET dependence in the proposed RBE model is significantly influenced by the cell type, where the cell type was represented by its α/β ratio of photons. The cell type was found to statistically significantly influence the LET–RBE relation.

A test that was not reported in Paper II but will be shown here is whether on the whole our developed RBE model for protons (model 1) gives a significantly better fit to the experimental data used in the study than the standard assumption of RBE equal to 1.1 (model 0). We assume normally distributed residuals ϵ and obtain the

likelihood for each model as

$$\mathcal{L} = \prod_i f(y_i \mid \theta) = \prod_i \frac{1}{\sigma\sqrt{2\pi}} e^{-\frac{\epsilon_i^2}{2\sigma^2}} \tag{46}$$

The test statistic V is obtained as

$$V = \frac{\ln(\mathcal{L}_1) - \ln(\mathcal{L}_0) - \frac{K_1 - K_0}{2}\ln(n)}{\sqrt{n\omega^2}} \tag{47}$$

where

$$\omega^2 = \frac{1}{n}\sum_{i=1}^{n} \ln\left(\frac{f_1(y_i \mid \theta_1)}{f_0(y_i \mid \theta_0)}\right)^2 \tag{48}$$

and n is the number of data points. K_1 and K_0 are the number of parameters in model 1 and 0, respectively. Vuong's test statistic follows a standard normal distribution, and the obtained value 3.24 corresponds to a two-tailed p-value equal to 0.001, indicating a stongly significantly better fit of the RBE model developed in Paper II than for the assumption of RBE equal to 1.1.

Resampling techniques

An alternative class of methods to estimate the precision and predictive value of a model on new data are resampling techniques. They attempt to mimic the process of new data generation, by drawing modified samples from the sample at hand.

Bootstrapping

Bootstrapping is a resampling technique first introduced by Efron (1979) that relies on sampling with replacement from the sample at hand, often using Monte Carlo methods. Traditionally, when one wants to draw conclusions about an aspect of an unknown population, inference requires assumptions about the distribution of the underlying data. The bootstrap analogy and fundamental assumption is that sampling with replacement from the original sample mimics the process of sampling from the underlying population. Thereby, the bootstrap eliminates the need to make strong assumptions about the distribution, such as normality. Instead, the assumption is that if the observed data is a representative sample of the population, conclusions can be made of the population by studying the sample. The bigger the

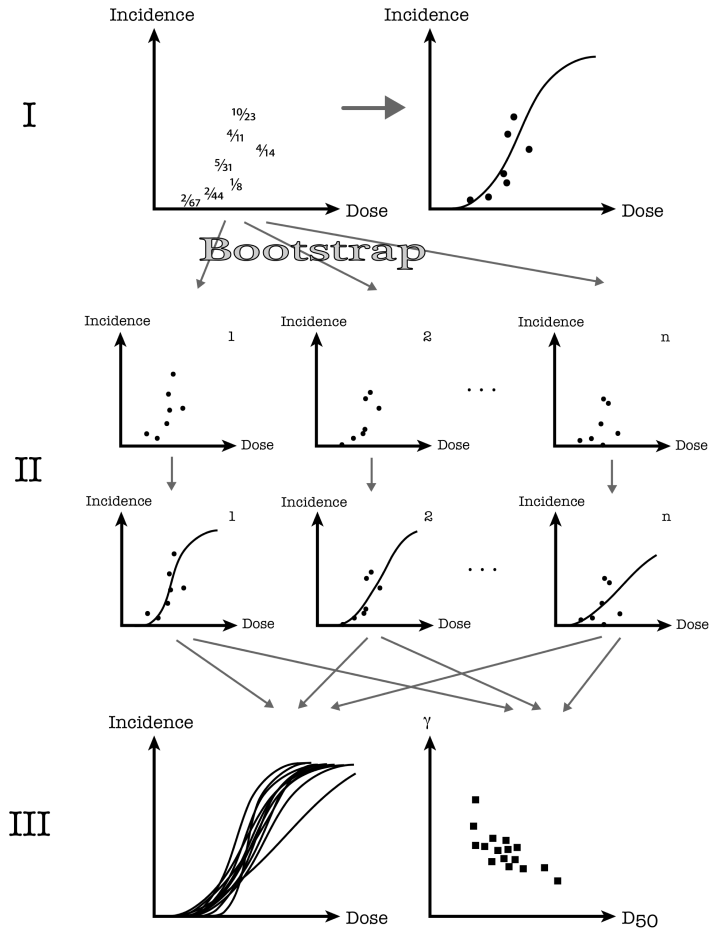

Figure 5: The bootstrap method. I: From the original incidence data given as the fraction of occurrences of the side effect of the total number of patients, an estimated dose-response relation can be obtained. II: Through sampling with replacement, plausible alternative outcomes at each dose are simulated. To each bootstrap replicate a dose-response curve is fitted. III: The resulting range of dose-response curves and model parameters visualizes the uncertainty due to sample variability.

original sample, the more likely it is to adequately reflect the nuances of the underlying population. Bootstrapping can be used for several purposes such as estimation of sampling variability, construction of (asymmetric) confidence intervals, and model selection.

From the observed data of size N, a new sample of the same size N is randomly drawn with replacement. Due to the replacement, each original data point may or may not be drawn and may be drawn more than once. This generates a bootstrap sample somewhat different from the original one. From this bootstrap sample some quantity of interest, such as the mean of a particular variable, a parameter estimate, or the goodness-of-fit, can be obtained and stored. The procedure is repeated to generate a large number (*e.g.* 10 000) bootstrap samples, and for each new sample the statistic of interest is computed. This provides a bootstrap distribution of the statistic from which standard errors, confidence intervals etc. can be obtained.

In Paper IV, a bootstrap method was proposed to assess the uncertainty of the outcome after irradiation of the lung (end point: pneumonitis) and spinal cord (end point: myelopathy). The data studied was obtained from the Quantitative Analysis of Normal Tissue Effects in Clinic (QUANTEC) review (Kirkpatrick et al., 2010; Marks et al., 2010). The QUANTEC report provides a summary of dose-response data for many types of normal tissue. Since the dose-response relations are estimated from limited numbers of patients, and recommendations of normal tissue constraints for radiation therapy are based on these relations, it is important to quantify the associated uncertainty. In Paper IV, the uncertainty due to sample variability was assessed. The QUANTEC report provides the number of patients, N_i, that received a certain dose to the organ studied, and how many of them experienced a certain side effect, in a particular study setting i. 10 000 bootstrap samples of the same size N_i as in the original data were produced by random sampling with replacement within each setting. For each bootstrap sample, the number of occurrences of the side effect was obtained. The result is a range of incidence estimates for a given dose. The procedure was repeated for all doses in the outcome data.

Two dose-response models, a Poisson-based linear model (17) and the Lyman model (20), were fitted to each bootstrapped dose-response relation using maximum likelihood estimation. The result is 10 000 dose-response curves for each model and as many sets of parameter values. The spread in the dose-response curves and parameter values reflect the uncertainty due to sample variability. An illustration of the bootstrap method is shown in Figure 5.

A 95% pointwise confidence band around the mean dose-response relation was obtained by ordering the model-based probability estimates for each dose unit and identifying the values at the lower and upper 2.5 percentiles.

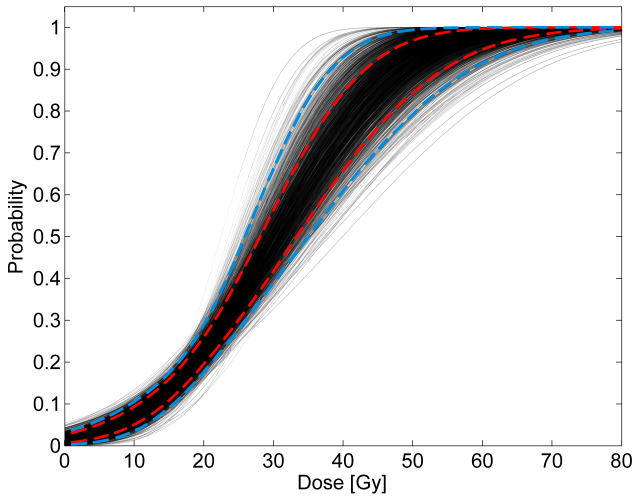

Figure 6: Dose-response curves for pneumonitis accounting for inter-experimental variation with 95% confidence interval (blue dashed lines). For comparison, the 95% confidence interval accounting only for variability within the studies are shown (red dashed lines).

The bootstrap method was used in Paper IV also for model selection. By comparing the maximum likelihood of the two dose-response models for each bootstrapped data set, the model selection relative frequencies can be determined. The model most often giving the best fit is considered the best. The Lyman model achieved higher maximum likelihood than the Poisson-based model in over 90% of the times for the outcome data of both spinal cord and lung. If the models to be compared have different number of parameters, AIC can be used as the criterion of selection instead of MLE.

The bootstrap analysis used in Paper IV was conditioned on the set of study settings in the original sample. Thereby, it resampled only the number of occurrences for each setting. Instead, one could have first resampled the study settings, and then resampled patients within each randomly drawn setting. This would reflect an additional source of variability – the composition of experimental settings in the original set of studies. The resulting range in dose-response curves is wider with this approach since it accounts both for variations within each experiment but also inter-experimental variation as shown in Figure 6. The method still provides a

lower limit on the total uncertainty since uncertainties in the delivered dose etc are not accounted for.

Cross validation

Cross validation is a model evaluation technique used to test a model's predictive ability on independent data. Predictive models require a proper trade-off between bias and variance, or with other words, between underfitting and overfitting to the data at hand. A model may give an accurate fit to the data it was fitted to but fail to perform on independent data from the same population. Too many parameters compared to the amount of data will generally result in a model with poor predictive power on new data. The result of overfitting is a model that describes random error or noise rather than the underlying relation.

A basic approach to test the generalization performance is to divide the data into a training set, to which the model is fitted, and a test set, against which the model is evaluated. This is referred to as hold-out testing. In Paper I, this approach was used to test the robustness of the developed LET-parameterized RCR model. The model was fitted to a subset of the cell survival data, and the model parameters estimated from this subset were subsequently evaluated against the excluded data. We found that the cell survival curves of the lowest LET, the highest LET, and the most effective LET for cell inactivation (at RBE maximum), could be used to predict the cell survival curves of all other LETs. In this study, the main interest was to evaluate the LET dependence of the model, and survival curves of pre-specified LETs were omitted in the robustness test. Another way of leaving data out would have been to randomly exclude individual data points from the cell survival data.

A problem with the hold-out method is that it is inefficient when the data set is small. The partitioning of the data results in less data available for building the model and can make the data set too small for accurate training. The hold-out method can be improved by repeating the process with different subsamples in so-called cross validation. In k-fold cross validation, the data is randomly divided into k subsets of equal size. k-1 subsets are pooled to form a training set and the remaining one is used for validation. The process is repeated k times with a different subset held out in each iteration. A special case of k-fold cross validation is when k equals the number of data points in the data. This method is called leave-one-out cross validation. A common choice is 10-fold cross validation. In the end, k values of the quantity used to measure performance are available, which can be averaged to obtain an aggregate measure. These measures can be used for model selection between competing models.

Treatment planning using biologically-based models

The aim in curative radiation therapy is to obtain local tumor control with high probability without too high risk of unacceptable side effects. In treatment planning, the clinical goals are instead usually stated indirectly in terms of physical quantities such as prescription dose and dose-volume limits to normal tissue. These quantities are used as surrogates of biological outcome instead of using estimates of biological outcome directly. An advantage of biological models is the more intuitive character which makes it easier to compare with clinical outcome, and that they more easily allow for including also the patient's own priorities in weighting different outcome probabilities.

The long use of radiation in the treatment of cancer has resulted in established clinical experience of the relation between dose and outcome for standard treatments. For example, keeping a maximum dose below a certain dose level to an organ has been correlated with an acceptable risk of side effects. Radiobiological models aim to capture this experience and make it explicit with mathematical expressions. Instead of threshold values, implying that an effect occurs above the stated criteria but not below, biologically-based metrics may provide continuous estimates of outcome probabilities. Since dose-volume based criteria only control a single point in the DVH, often several functions are required for an organ, and individual priorities between these may be needed. Biologically-based cost functions have the advantage that they comprise the entire dose distribution and provide an inherent prioritization of the dose-volume domain. Biological models are also useful in plan comparison. It can be difficult to judge and order different plans only based on dose distributions and DVHs.

Biological models are valuable for standard treatment but are even more needed when deviations from the intended treatment are made. If the treatment of a

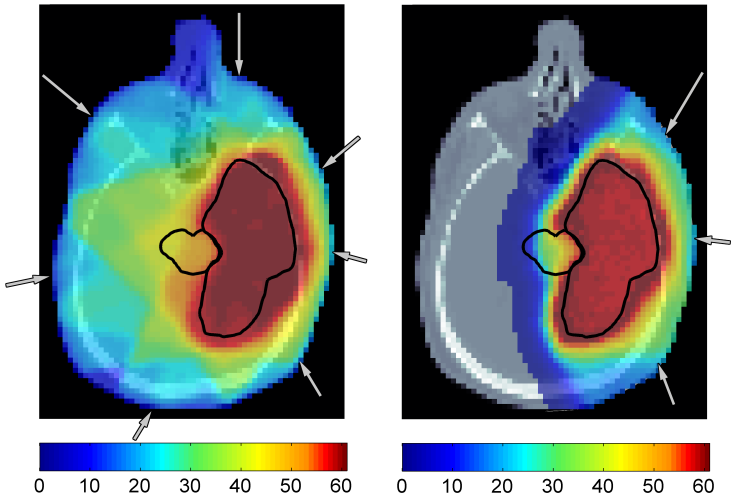

Figure 7: The left panel shows the dose distribution of the total dose (Gy) for the IMRT plan, and the right panel shows the RBE-weighted dose distribution for the IMPT plan accounting for a variable RBE. The arrows show beam angles.

patient is changed for some reason, for example dose fractions are missed due to the patient being absent or the treatment machine going down, the total dose cannot be used alone to determine the outcome. Another scenario is that deviations from the intended dose distribution, due to organ motion or tumor shrinkage, are detected from imaging during the course of treatment. Biological models are then needed to calculate how to compensate for the deviations. For protons, and even more so for carbon ions, the dose alone is even more difficult to use as a predictor for outcome.

In Paper III, two treatment plans for a brain tumor case were compared (see Figure 7). The tumor was located close to critical organs such as the brain stem and optic nerve. Both plans were created using intensity modulated beams, one using photons (IMRT) and one using protons (IMPT). Since equal physical photon and proton doses do not give equal biological effect, a plan comparison based on doses cannot be made directly. In this study, the proton dose was converted to a biologically equivalent photon dose using RBE. In the optimization of the proton plan, a standard constant RBE equal to 1.1 was assumed. In the plan evaluation, both a standard RBE of 1.1 and an RBE distribution calculated using the RBE-

model (34) developed in Paper II were used to weight the physical dose obtained in the plan creation.

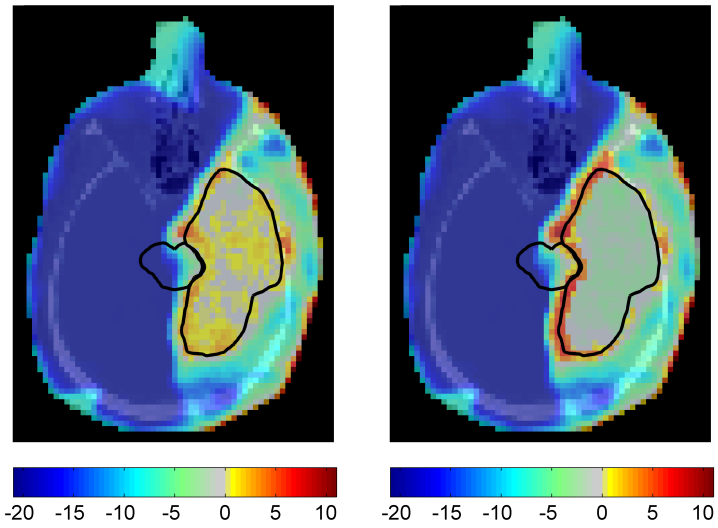

Figure 8: The left panel shows the difference in equivalent doses between the IMPT plan and the IMRT plan under the standard assumption of RBE equal to 1.1 (proton $RBE_{1.1}$-weighted dose - photon dose). The right panel shows the dose difference when accounting for variable RBE.

The plan comparison showed that considerably lower equivalent doses to normal tissues were generally obtained with protons compared to photons regardless of the RBE assumed. However, the DVH revealed so called hot spots, high doses in small volumes, in the proton plan. Even with the knowledge that brain stem and optic nerve are serial organs where the highest doses to a high extent determine the outcome, it is difficult to know where trade-off lies. How ”hot” do the hot spots in an organ need to be to override the favorable low doses everywhere else? The NTCP model (22) used predicts that the very limited hot spots in for example the brain stem estimated with an RBE equal to 1.1, did not overcome the much lower dose to this organ in general compared to the plan obtained with photons. A lower NTCP was estimated in the proton plan compared to the photon plan. In contrast, when a variable RBE was accounted for, the hot spots generated a predicted worse NTCP for the brain stem with protons compared to photons, despite the otherwise

much lower dose.

For the tumor, a somewhat higher biological equivalent dose in the tumor was obtained with protons compared to photons under the assumption of RBE equal to 1.1, whereas the opposite was obtained under the evaluation accounting for RBE variation. Figure 8 show the difference in equivalent doses between protons and photons calculated using both RBE equal to 1.1 and a variable RBE. In conclusion, the RBE model predicts a disadvantageous trend with lower biological effect in the tumor (high α/β) and higher effect in late-responding normal tissue (low α/β) than expected from the standard assumption of a constant RBE equal to 1.1.

In the study presented in Paper III, the plans were optimized based on dose and dose-volume functions with an assumed RBE equal to 1.1. Only the evaluation was based on biological models. If the plans were optimized using also biological models, possibly a better proton plan could have been obtained.

Models describing the relationship between dose, irradiated volume and tissue response are associated with uncertainties because of the difficulty to precisely assess the reaction of tumors and surrounding normal tissues to radiation. These uncertainties and model limitations have so far restricted the application of biologically based optimization methods in clinical radiation therapy. Today, biological models can be useful in optimizing and evaluating treatment plans, but should not be relied upon uncritically. Especially not if they suggest non-standard treatments. Instead biological and physical criteria should be used together.

Summary of papers

Paper I: Analytical description of the LET dependence of cell survival using the repairable-conditionally repairable damage model

Paper I is co-authored with Bengt K. Lind, Iuliana Toma-Dasu, Henrik Rehbinder, and Anders Brahme, and has been published in Radiation Research, Vol. 174, pp. 517-525, 2010.

In this paper, we extend the repairable-conditionally repairable (RCR) damage model by including an LET-parameterization to provide a radiobiological model for ions that accounts for both dose and LET. The LET dependence is incorporated by expressing the model's parameters as functions of LET. These expressions are derived so that the model agrees with expected biological mechanisms.

The model was found to fit published cell survival data irradiated with helium ions and carbon ions for LETs ranging up to LETs high enough to observe a reduced effectiveness in cell inactivation per unit dose, the so-called overkill effect. The model's ability to predict unseen experimental data using only a limited subset of the experimental data was evaluated, and the excluded data could indeed be recreated. The fraction of cells being damaged decreases at high LETs for a constant dose level, which could be explained by a clustering of damage in some cells at the expense of other cells being non-hit, and the normalized fraction of cells being repaired decreases with increasing LET.

By expressing the parameters as functions of LET instead of having these parameters free, and by fitting the cell survival curves of all LETs simultaneously instead of making an individual fit for each LET, a somewhat less accurate fit to the data is obtained. The gain is the generalization that opens up the possibility of estimating cell survival also for dose and LET combinations for which we have no experimental data available.

Paper II: A model for the relative biological effectiveness of protons: The tissue specific parameter α/β of photons is a predictor for the sensitivity to LET changes

Paper II is co-authored with Bengt K. Lind and Björn Hårdemark, and has been published in Acta Oncologica, Vol 52, pp 580-588, 2013.

In this paper, we propose a model for the relative biological effectiveness (RBE) of protons where RBE variations due to LET, dose, and cell type are accounted for. The RBE model is based on the linear-quadratic model, and the cell type is represented by the $(\alpha/\beta)_{\text{phot}}$ ratio of the reference photon radiation. Published α and β parameters of the LQ model obtained after proton irradiated were studied with respect to their dependence of LET. Clonogenic cell survival data of ten different cell lines irradiated with near monoenergetic proton beams with LET values ranging from 6 to 30 keV/μm was selected.

A statistically significant positive relation between $\alpha/\alpha_{\text{phot}}$ and LET was found. However, upon a closer examination, it was the cell lines with low $(\alpha/\beta)_{\text{phot}}$ that contributed to the positive slope. The slope was found to vary statistically significantly with $(\alpha/\beta)_{\text{phot}}$. No statistically significant relation was found between $\beta/\beta_{\text{phot}}$ and LET.

The proposed model predicts a cell-dependent relation between RBE and LET determined by the $(\alpha/\beta)_{\text{phot}}$ ratio: RBE increases with increasing LET for cell lines with low $(\alpha/\beta)_{\text{phot}}$ ratio, but the relation becomes weaker with increasing $(\alpha/\beta)_{\text{phot}}$, and at high $(\alpha/\beta)_{\text{phot}}$ ratios, RBE is low and relatively insensitive to LET changes. This implicates that late-responding tissues are more sensitive to high LETs than early-responding tissues and most tumors. Moreover, the model shows an increasing RBE with decreasing dose per fraction in a cell-dependent way, where the effect is most pronounced for low $(\alpha/\beta)_{\text{phot}}$.

In conclusion, the $(\alpha/\beta)_{\text{phot}}$ ratio describing the sensitivity of cells to photon radiation, is a predictor also for the sensitivity to proton radiation. The highest RBE values are predicted for cell lines with low $(\alpha/\beta)_{\text{phot}}$ receiving high LET and low dose per fraction.

Paper III: Disregarding RBE variation in treatment plan comparison may lead to bias in favor of proton therapy

Paper III is co-authored with Iuliana Toma-Dasu, and has been submitted for publication.

In this study, the aim is to investigate how the comparison of treatment plans created using photons and protons is affected by accounting for a variable RBE. When comparing treatment plans of protons and photons, the increased effectiveness of protons per unit dose has to be taken into account and biologically equivalent doses should be used. The conversion from a physical proton dose into an equivalent photon dose is made by the concept of RBE. In clinics today, the RBE is usually assumed to be constant and equal to 1.1. However, proton RBE has experimentally been found to depend on various factors. In this study, the effect of disregarding RBE variations is evaluated.

Two intensity modulated treatment plans, one using photons (IMRT) and one using protons (IMPT), were created for the same patient. In this brain tumor case the tumor is located close to the brain stem and optic nerve. The proton plan was optimized with a standard RBE equal to 1.1 with the aim to produce a plan giving as high dose to the tumor as the photon plan or higher while limiting the dose to normal tissues to be as low as in the photon plan or lower. In the plan comparison, a variable RBE was accounted for. The RBE model developed in Paper II was used. To calculate an RBE distribution, the LET distribution is needed. The LET calculation was implemented in the Monte Carlo dose engine framework for pencil beam scanning in the treatment planning system RayStation (RaySearch Laboratories, Stockholm, Sweden). For each voxel, the contributions from all protons were scored, and a dose averaged LET was calculated.

Under the assumption of RBE equal to 1.1, higher equivalent doses to the tumor were obtained for the proton plan compared to the photon plan while the equivalent dose to the normal tissues was lower. In contrast, when accounting for RBE variations, the comparison showed lower equivalent doses to the tumor and hot spots in organs at risk in the proton plan. These hot spots resulted in higher estimated NTCPs in the proton plan compared to the photon plan under the assumption of variable RBE. Disregarding RBE variations, might lead to a lower effect in the tumor and a higher effect in normal tissues than expected. This trend may lead to bias in favor of proton therapy in the comparison with photon therapy.

Paper IV: Assessing the uncertainty in QUANTEC's dose-response relation of lung and spinal cord with a bootstrap analysis

Paper IV has been accepted for publication in International Journal of Radiation Oncology, Biology, Physics.

Dose-response relations are typically estimated from limited numbers of patients, rendering the relation uncertain. In this paper, we apply a bootstrap method to assess the uncertainty of estimated population-based dose-response relations due to sample variability.

Two clinical dose-response relations presented by QUANTEC, myelopathy of the cervical spinal cord and pneumonitis, were studied. The bootstrap method generates a range of plausible outcome probabilities by random sampling with replacement from the original incidence data. The uncertainty in the clinical outcome data was translated into an uncertainty in the dose-response relation described by two commonly used models: the Poisson-based model and the Lyman model.

A 95% confidence interval for the mean dose-response was created as well as a 95% confidence area of the resulting model parameter distribution. The Lyman model showed a steeper slope than the Poisson-based model, and the model parameter pairs indicated correlation and non-Gaussian distribution. The bootstrap model selection method preferred the Lyman model over the Poisson-based model. The Lyman model had higher likelihood in over 90% of the bootstrap replicates in both the lung case and the spinal cord case.

In conclusion, the proposed bootstrap method enables statistical analysis of the uncertainty of the estimated dose-response relations based on the variability inherent in the incidence data from which they are derived.

Conclusions and outlook

In this project, two mathematical models for biological effect estimation for ions have been developed. In Paper I, the RCR cell survival model was extended to account for LET. The LET-parameterized RCR model was found to be applicable for estimating experimental cell survival data obtained from irradiation with carbon ions and helium ions. The model predicts a decreasing survival probability with increasing LET, but also accounts for the lower efficiency for further increased LET, the overkill effect. The analytically expressed LET dependence allows for predictions of survival probability for dose-LET combinations for which there is no experimental data, and facilitates optimization.

The second model was developed specifically for protons and estimates the RBE based on dose, LET, and cell type. The proposed model predicts a cell-dependent relation between RBE and LET determined by the α/β ratio of photons. In general, RBE increases with increasing LET, but the strength of the relation decreases with increasing α/β. The highest RBE values are predicted for cell lines with low α/β receiving high LET and low dose per fraction. The model was found to provide adequate fit to experimental RBE data obtained at 2 Gy photon dose for various cell types and LET values.

The derived RBE model was applied to a realistic treatment scenario. The model predicted a lower RBE than the commonly assumed value of 1.1 in the brain tumor studied, and higher RBE than 1.1 in critical organs close to the tumor. As a consequence, a treatment plan derived under the assumption of an RBE equal to 1.1 gave lower than expected effect in the tumor and higher than expected effect in normal tissue, provided that the trends of our model are correct. We showed that disregarding RBE variation may lead to bias in favor of proton therapy in comparison to photon therapy.

Different methods for evaluating radiobiological models have been proposed and used. A hold-out method was used in Paper I to test the ability of the LET-parameterized RCR model to estimate survival curves for excluded LETs. Statisti-

cal hypothesis tests, including Vuong's test, were used in Paper II in the development of the RBE model. In Paper IV, a bootstrap method was proposed to evaluate two dose-response models: the Lyman model and a Poisson-based model. With the current amount of clinical toxicity studies, typically with limited number of patients included in each, sampling variability is of fundamental importance. The uncertainty of the empirically derived biological models must be acknowledged and accounted for in their application. The proposed bootstrap framework provides a generally applicable method to evaluate the uncertainty of radiobiological models due to sampling variability. The method provides confidence intervals of the dose-response relation, model parameter values with confidence intervals and their interrelation, and can be used for model selection.

This thesis makes contributions to the methodology for biological effect estimation with mathematical models. Ultimately, these models could assist in the search for optimal treatment plans. A specific challenge for research and method development in this area is the limited amount of available data. Model development and evaluation requires good and abundant empirical data. An important priority for the future should be to collect data and ensure that it can be shared within the research community. More detailed data should be presented in scientific publications, in order that the results can be reproduced and re-evaluated. Specifically, effective use of methods such as the bootstrap requires access to the original data points; sample means and variances do not suffice.

Radiobiological models can potentially direct optimization toward clinically advantageous treatments, but the uncertainties of the models and their parameters have so far restricted their use. In Paper IV, the uncertainty due to sampling variability was assessed and applied to dose-response relations, and confidence intervals for model parameters were derived. With information about the full dose distribution, the same approach could be used to estimate the uncertainty of predicted dose-volume effects. A step forward in biology-based treatment planning would be to account for uncertainties in model parameters by incorporating them into objective functions for robust optimization. In this way, conservative predictions of clinical outcome probabilities, such as worst case scenarios, could be produced.

To utilize the full potential of protons in radiation therapy, treatment plans should be optimized not only based on dose distribution, but also based on LET. Biological models are needed in order to do so, since the dependence between biological effect and LET varies with the type of tissue. The impact of the RBE model developed in Paper II on treatment plan comparison was evaluated in Paper III. A natural next step would be to implement the RBE model into a treatment planning system for use in treatment plan optimization.

Acknowledgements

The work presented in this thesis has been carried out as a joint project between the Department of Oncology-Pathology, Division of Medical Radiation Physics, at Karolinska Institutet, and RaySearch Laboratories. The project was co-funded by RaySearch Laboratories and the Swedish Research Council (Vetenskapsrådet).

I would like to express my gratitude to all those who have supported me during my PhD studies. In particular, I would like to thank:

Bengt Lind, my main advisor, for scientific guidance and encouragement throughout these years, and for putting trust in my capability. I appreciate your open-minded and helpful attitude.

Iuliana Toma-Dasu, my co-advisor, for invaluable comments, and interesting and rewarding discussions. Your ability to work thoroughly *and* fast is impressive! I am grateful for your active assistance in all possible matters, and for always taking your time.

Björn Hårdemark, my co-advisor and head of research at RaySearch, for advice and insightful comments, and for sharing your vast knowledge in radiation therapy. I admire your genuine interest in solving real world problems.

Anders Brahme, for advising me during the first years of the project. Thank you for welcoming me to your research group and for your great enthusiasm for my work and for science in general. It has been a privilege working with you!

Henrik Rehbinder, my co-advisor during the first years of the project, for encouragement and guidance, and inspiration to broaden my scientific perspective.

Johan Löf, the founder and CEO of RaySearch, for directing my research project towards the interesting fields of ion therapy and radiation biology, and for your strong support and leadership.

My other colleagues at **RaySearch** for making this such an inspiring and fun place to work at. Especially, I would like to thank: **Kjell Eriksson** for enjoyable discussions and collaborations on biology-related projects, and for guiding me around in the CoreOrbit programming code. Du är en ljus glödlampa! **Tore Ers-**

mark for introducing me to the proton Monte Carlo code, and for helping me decipher compilation error messages. **Erik Traneus** and **Martin Janson** for always taking your time for discussions about LET and proton physics. Many thanks also to **Albin Fredriksson**, **Rasmus Bokrantz**, and **Elin Hynning**, my roommates, for your helpfulness and good spirit.

All past and present faculty members at the **Division of Medical Radiation Physics (MSF)**, Karolinska Institutet, for interesting discussions and seminars. A special thanks to **Margareta Edgren** for generously sharing your vast knowledge in radiation biology, and **Bo Nilsson** for excellent teaching in radiation physics. Fellow PhD students **Marta Lazzeroni, Eleftheria Alevronta, Laura Antonovic, Thiansin Liamsuwan, Reza Taleei, Tommy Sundström, Kristin Wiklund, Martha Hultqvist, Johanna Kempe, Björn Andreassen, Sara Janek Stråat, Patrick Vreede, Till Böhlen, Bahram Andisheh, Katarzyna Zielinska-Chomej, Chitralekha Mohanty, Soyoung Kim, Rickard Holmberg, Malin Siddiqi, Magdalena Adamus-Gorka, Bartosz Gorka, Malin Hollmark** - thank you for all the good times we had!

Nina Tilly and **Bo Stenerlöw** for valuable feedback on my half-time seminar.

Ulf Isacsson for kindly inviting me to Akademiska sjukhuset and The Svedberg Laboratoriet in Uppsala, and showing me how radiation therapy with x-rays and protons, and brachytherapy, is performed in practice. I learned a lot!

Björn Cedervall for accepting to examine me in radiation biology on such short notice, and for inviting me to Vattenfall.

Johan Åqvist and **Jens Carlsson** from the Division of Computational and Systems Biology at the Department of Cell and Molecular Biology at Uppsala University, and **Sandra Visser** from AstraZeneca, for providing me with the first opportunities to do research on mathematical models of biological systems.

My warmest thanks to friends and family. A special thanks to **Christina** and **Hans-Göran** for being wonderful parents-in-law. You are such warm-hearted persons! My parents **Maija** and **Kaj**, you are the source of my interest in biology and medical science. I am grateful for all our discussions, and for your everlasting support and encouragement.

Finally, the most important persons: **Niklas**, my husband, my love. I cannot thank you enough for all your support in every possible way. But most of all, for your love and for being my best friend. And **Oliver** and **Ville**, our wonderful children. You make my life brighter!

Stockholm, August 2013
Minna Wedenberg

References

Ahnesjö, A., Hårdemark, B., Isacsson, U., and Montelius, A. (2006). The IMRT information process–mastering the degrees of freedom in external beam therapy. *Physics in medicine and biology*, 51(13):R381.

Akaike, H. (1973). Information theory and an extension of the maximum likelihood principle. In *Second international symposium on information theory*, pages 267–281. Akademinai Kiado.

Allen, C., Borak, T. B., Tsujii, H., and Nickoloff, J. A. (2011). Heavy charged particle radiobiology: using enhanced biological effectiveness and improved beam focusing to advance cancer therapy. *Mutation Research/Fundamental and Molecular Mechanisms of Mutagenesis*, 711(1):150–157.

Barendsen, G. (1982). Dose fractionation, dose rate and iso-effect relationships for normal tissue responses. *International Journal of Radiation Oncology* Biology* Physics*, 8(11):1981–1997.

Belli, M., Cera, F., Cherubini, R., Dalla Vecchia, M., Haque, A., Ianzini, F., Moschini, G., Sapora, O., Simone, G., Tabocchini, M., and Tiveron, P. (1998). RBE-LET relationships for cell inactivation and mutation induced by low energy protons in V79 cells: further results at the LNL facility. *International Journal of Radiation Biology*, 74(4):501–509.

Bokrantz, R. (2013). *Multicriteria Optimization for Managing Tradeoffs in Radiation Therapy Treatment Planning*. PhD thesis, KTH Royal Institute of Technology.

Bortfeld, T. (2006). IMRT: a review and preview. *Physics in medicine and biology*, 51(13):R363.

Box, G. E. and Draper, N. R. (1987). *Empirical model-building and response surfaces.* John Wiley & Sons.

Brahme, A. (1984). Dosimetric precision requirements in radiation therapy. *Acta Oncologica*, 23(5):379–391.

Brahme, A. (1988). Optimization of stationary and moving beam radiation therapy techniques. *Radiotherapy and Oncology*, 12(2):129–140.

Brahme, A. (2004). Recent advances in light ion radiation therapy. *International Journal of Radiation Oncology* Biology* Physics*, 58(2):603–616.

Brahme, A., Roos, J.-E., and Lax, I. (1982). Solution of an integral equation encountered in rotation therapy. *Physics in medicine and biology*, 27(10):1221.

Brenner, D. J. and Hall, E. J. (1999). Fractionation and protraction for radiotherapy of prostate carcinoma. *International Journal of Radiation Oncology* Biology* Physics*, 43(5):1095–1101.

Burnham, K. P. and Anderson, D. R. (2002). *Model selection and multi-model inference: A practical information-theoretic approach*. Springer.

Cancerfonden (accessed: August 2013, updated: June 2013). Cancer i siffror 2013, http://www.cancerfonden.se.

Carabe, A., Moteabbed, M., Depauw, N., Schuemann, J., and Paganetti, H. (2012). Range uncertainty in proton therapy due to variable biological effectiveness. *Physics in medicine and biology*, 57(5):1159.

Castro, J. R., Linstadt, D. E., Bahary, J.-P., Petti, P. L., Daftari, I., Collier, J. M., Gutin, P. H., Gauger, G., and Phillips, T. L. (1994). Experience in charged particle irradiation of tumors of the skull base: 1977–1992. *International Journal of Radiation Oncology* Biology* Physics*, 29(4):647–655.

Castro, J. R., Saunders, W. M., Tobias, C. A., Chen, G. T., Curtis, S., Lyman, J. T., Michael Collier, J., Pitluck, S., Woodruff, K. A., Blakely, E. A., et al. (1982). Treatment of cancer with heavy charged particles. *International Journal of Radiation Oncology* Biology* Physics*, 8(12):2191–2198.

Chadwick, K. and Leenhouts, H. (1973). A molecular theory of cell survival. *Physics in Medicine and Biology*, 18(1):78.

Combs, S. E., Jäkel, O., Haberer, T., and Debus, J. (2010). Particle therapy at the Heidelberg Ion Therapy Center (HIT)–Integrated research-driven university-hospital-based radiation oncology service in Heidelberg, Germany. *Radiotherapy and Oncology*, 95(1):41–44.

Curtis, S. B. (1986). Lethal and potentially lethal lesions induced by radiation–A unified repair model. *Radiation Research*, 106(2):252–270.

Dale, R. and Jones, B. (2007). *Radiobiological modelling in radiation oncology*. British Institute of Radiology, London, UK.

Dale, R. G. (1985). The application of the linear-quadratic dose-effect equation to fractionated and protracted radiotherapy. *British Journal of Radiology*, 58(690):515–528.

Dale, R. G. and Jones, B. (1999). The assessment of RBE effects using the concept of biologically effective dose. *International Journal of Radiation Oncology* Biology* Physics*, 43(3):639–645.

Dasu, A. and Toma-Dasu, I. (2012). Prostate alpha/beta revisited – an analysis of clinical results from 14 168 patients. *Acta Oncologica*, 51(8):963–974.

Efron, B. (1979). Bootstrap methods: another look at the jackknife. *The annals of Statistics*, pages 1–26.

Elsässer, T., Krämer, M., and Scholz, M. (2008). Accuracy of the Local Effect Model for the prediction of biologic effects of carbon ion beams in vitro and in vivo. *International Journal of Radiation Oncology* Biology* Physics*, 71(3):866–872.

Elsässer, T. and Scholz, M. (2007). Cluster effects within the Local Effect Model. *Radiation Research*, 167:319–329.

Elsässer, T., Weyrather, W. K., Friedrich, T., Durante, M., Iancu, G., Krämer, M., Kragl, G., Brons, S., Winter, M., Weber, K.-J., et al. (2010). Quantification of the relative biological effectiveness for ion beam radiotherapy: direct experimental comparison of proton and carbon ion beams and a novel approach for treatment planning. *International Journal of Radiation Oncology* Biology* Physics*, 78(4):1177–1183.

Fokas, E., Kraft, G., An, H., and Engenhart-Cabillic, R. (2009). Ion beam radiobiology and cancer: time to update ourselves. *Biochimica et Biophysica Acta (BBA)-Reviews on Cancer*, 1796(2):216–229.

Fowler, J. (2010). 21 years of biologically effective dose. *British Journal of Radiology*, 83(991):554–568.

Fowler, J. F., Toma-Dasu, I., and Dasu, A. (2013). Is the α/β ratio for prostate tumours really low and does it vary with the level of risk at diagnosis? *Anticancer research*, 33(3):1009–1011.

Fredriksson, A. (2013). *Robust optimization of radiation therapy accounting for geometrical uncertainties*. PhD thesis, KTH Royal Institute of Technology.

Frese, M. C., Yu, V. K., Stewart, R. D., and Carlson, D. J. (2012). A mechanism-based approach to predict the relative biological effectiveness of protons and carbon ions in radiation therapy. *International Journal of Radiation Oncology* Biology* Physics*, 83(1):442–450.

Gerweck, L. E. and Kozin, S. V. (1999). Relative biological effectiveness of proton beams in clinical therapy. *Radiotherapy and oncology*, 50(2):135–142.

Goitein, M. (2008). *Radiation oncology: A physicist's-eye view*. Springer, New York.

Goodhead, D. t. (1994). Initial events in the cellular effects of ionizing radiations: clustered damage in DNA. *International journal of radiation biology*, 65(1):7–17.

Hall, E. J. (2006). Intensity-modulated radiation therapy, protons, and the risk of second cancers. *International Journal of Radiation Oncology* Biology* Physics*, 65(1):1–7.

Hall, E. J. and Giaccia, A. J. (2006). *Radiobiology for the Radiologist*. Lippincott Williams and Wilkins.

Hastie, T., Tibshirani, R., and Friedman, J. (2009). *The elements of statistical learning: Data mining, inference, and prediction*. Springer.

Hawkins, R. B. (1998). A microdosimetric-kinetic theory of the dependence of the RBE for cell death on LET. *Medical physics*, 25:1157.

ICRU (1970). *ICRU Report 16: Linear Energy Transfer*. International Commission on Radiation Units and Measurements, Washington.

ICRU (1980). *ICRU Report 33: Radiation quantities and units*. International Commission on Radiation Units and Measurements, Bethesda.

ICRU (2007). Radiation biology considerations. In *ICRU Report 78: Prescribing, Recording, and Reporting Proton-Beam Therapy*. Oxford University Press, Oxford.

Jackson, S. P. (2002). Sensing and repairing DNA double-strand breaks. *Carcinogenesis*, 23(5):687–696.

Joiner, M. and Johns, H. (1988). Renal damage in the mouse: the response to very small doses per fraction. *Radiation research*, 114(2):385–398.

Joiner, M. C., Marples, B., Lambin, P., Short, S. C., and Turesson, I. (2001). Low-dose hypersensitivity: current status and possible mechanisms. *International Journal of Radiation Oncology* Biology* Physics*, 49(2):379–389.

Jones, B. (2008). The potential clinical advantages of charged particle radiotherapy using protons or light ions. *Clinical Oncology*, 20(7):555–563.

Jones, B., Dale, R., Deehan, C., Hopkins, K., and Morgan, D. (2001). The role of biologically effective dose (BED) in clinical oncology. *Clinical Oncology*, 13(2):71–81.

Källman, P., Lind, B., and Brahme, A. (1992). An algorithm for maximizing the probability of complication-free tumour control in radiation therapy. *Physics in medicine and biology*, 37(4):871.

Kanai, T., Endo, M., Minohara, S., Miyahara, N., Koyama-ito, H., Tomura, H., Matsufuji, N., Futami, Y., Fukumura, A., Hiraoka, T., et al. (1999). Biophysical characteristics of HIMAC clinical irradiation system for heavy-ion radiation therapy. *International Journal of Radiation Oncology* Biology* Physics*, 44(1):201–210.

Kanai, T., Furusawa, Y., Fukutsu, K., Itsukaichi, H., Eguchi-Kasai, K., and Ohara, H. (1997). Irradiation of mixed beam and design of spread-out bragg peak for heavy-ion radiotherapy. *Radiation research*, 147(1):78–85.

Karlsson, K. H. and Stenerlöw, B. (2004). Focus formation of DNA repair proteins in normal and repair-deficient cells irradiated with high-LET ions. *Radiation research*, 161(5):517–527.

Kellerer, A. M. and Rossi, H. H. (1978). A generalized formulation of dual radiation action. *Radiation Research*, 75(3):471–488.

Kirkpatrick, J. P., Brenner, D. J., and Orton, C. G. (2009). The linear-quadratic model is inappropriate to model high dose per fraction effects in radiosurgery. *Medical physics*, 36:3381.

Kirkpatrick, J. P., van der Kogel, A. J., and Schultheiss, T. E. (2010). Radiation dose–volume effects in the spinal cord. *International Journal of Radiation Oncology* Biology* Physics*, 76(3):S42–S49.

Kraft, G. (2000). Tumor therapy with heavy charged particles. *Progress in Particle and Nuclear Physics*, 45:S473–S544.

Krämer, M. and Scholz, M. (2000). Treatment planning for heavy-ion radiotherapy: calculation and optimization of biologically effective dose. *Physics in medicine and biology*, 45(11):3319.

Kutcher, G. J. and Burman, C. (1989). Calculation of complication probability factors for non-uniform normal tissue irradiation: The effective volume method. *International Journal of Radiation Oncology* Biology* Physics*, 16(6):1623–1630.

Lea, D. (1946). Actions of radiations on living cells. *University Press, Cambridge*.

Lea, D. and Catcheside, D. (1942). The mechanism of the induction by radiation of chromosome aberrations in tradesoantia. *Joumal of Genetics*, 44:216–245.

Lind, B., Persson, L., Edgren, M., Hedlöf, I., and Brahme, A. (2003). Repairable-conditionally repairable damage model based on dual poisson processes. *Radiation research*, 160(3):366–375.

Lind, B. K., Mavroidis, P., Hyödynmaa, S., and Kappas, C. (1999). Optimization of the dose level for a given treatment plan to maximize the complication-free tumor cure. *Acta Oncol.*, 38(6):787–798.

Lyman, J. T. (1985). Complication probability as assessed from dose-volume histograms. *Radiation Research*, 104(2s):S13–S19.

Marks, L. B., Bentzen, S. M., Deasy, J. O., Kong, F.-M. S., Bradley, J. D., Vogelius, I. S., El Naqa, I., Hubbs, J. L., Lebesque, J. V., Timmerman, R. D., et al. (2010). Radiation dose–volume effects in the lung. *International Journal of Radiation Oncology* Biology* Physics*, 76(3):S70–S76.

Monz, M., Küfer, K., Bortfeld, T., and Thieke, C. (2008). Pareto navigation-algorithmic foundation of interactive multi-criteria IMRT planning. *Physics in medicine and biology*, 53(4):985.

Niemierko, A. (1997). Reporting and analyzing dose distributions: a concept of equivalent uniform dose. *Medical physics*, 24:103.

Niemierko, A. (1999). A generalized concept of equivalent uniform dose (EUD). *Medical Physics*, 26:1100.

Prise, K. M. and O'Sullivan, J. M. (2009). Radiation-induced bystander signalling in cancer therapy. *Nature Reviews Cancer*, 9(5):351–360.

PTCOG (accessed August 2013, updated March 2013). Particle Therapy Co-Operative Group, http://ptcog.web.psi.ch.

Saunders, W., Castro, J., Chen, G., Collier, J., Zink, S., Pitluck, S., Phillips, T., Char, D., Gutin, P., Gauger, G., et al. (1985). Helium-ion radiation therapy at the Lawrence Berkeley Laboratory: Recent results of a Northern California Oncology Group clinical trial. *Radiation Research*, 104(2s):S227–S234.

Scholz, M., Kellerer, A., Kraft-Weyrather, W., and Kraft, G. (1997). Computation of cell survival in heavy ion beams for therapy. *Radiation and environmental biophysics*, 36(1):59–66.

Schulz-Ertner, D., Jäkel, O., and Schlegel, W. (2006). Radiation therapy with charged particles. *Semin Radiat Oncol*, 16(4):249–59.

Schwarz, G. (1978). Estimating the dimension of a model. *The annals of statistics*, 6(2):461–464.

Sinclair, W. (1966). The shape of radiation survival curves of mammalian cells cultured in vitro. *Biophysical aspects of radiation quality*, pages 21–43.

Sontag, W. (1997). A discrete cell survival model including repair after high dose-rate of ionizing radiation. *International journal of radiation biology*, 71(2):129–144.

Tilly, N., Johansson, J., Isacsson, U., Medin, J., Blomquist, E., Grusell, E., and Glimelius, B. (2005). The influence of RBE variations in a clinical proton treatment plan for a hypopharynx cancer. *Physics in medicine and biology*, 50(12):2765.

Tobias, C. A. (1985). The repair-misrepair model in radiobiology: Comparison to other models. *Radiation Research*, 104(2s):S77–S95.

Toma-Dasu, I. and Dasu, A. (2013). Modelling tumour oxygenation, reoxygenation and implications on treatment outcome. *Computational and mathematical methods in medicine*, 2013.

Unkelbach, J., Bortfeld, T., Martin, B. C., and Soukup, M. (2009). Reducing the sensitivity of IMPT treatment plans to setup errors and range uncertainties via probabilistic treatment planning. *Medical physics*, 36:149.

Vaupel, P. and Mayer, A. (2007). Hypoxia in cancer: significance and impact on clinical outcome. *Cancer and Metastasis Reviews*, 26(2):225–239.

Vuong, Q. H. (1989). Likelihood ratio tests for model selection and non-nested hypotheses. *Econometrica: Journal of the Econometric Society*, pages 307–333.

Weyrather, W. and Debus, J. (2003). Particle beams for cancer therapy. *Clinical Oncology*, 15(1):S23–S28.

WHO (accessed August 2013, updated January 2013). World Health Organization, http://www.who.int/cancer.

Wilkens, J. and Oelfke, U. (2004). A phenomenological model for the relative biological effectiveness in therapeutic proton beams. *Physics in medicine and biology*, 49(13):2811.

Wilson, R. R. et al. (1946). Radiological use of fast protons. *Radiology*, 47(5):487–491.

Withers, R., Taylor, J. M., and Maciejewski, B. (1988). Treatment volume and tissue tolerance. *International Journal of Radiation Oncology* Biology* Physics*, 14(4):751–759.